Velocity overshoot for incompressible flows past a semi-infinite flat plate

Daniela Capatina, Didier Graebling, Robert Luce, David Trujillo

Velocity overshoot for incompressible flows past a semi-infinite flat plate

Daniela Capatina, Didier Graebling, Robert Luce, and David Trujillo,

Université de Pau, Laboratoire de Mathématiques et de leurs Applications - UMR CNRS 5142.

September 21, 2021. :1–30

Keywords

Boundary layer theory, velocity overshoot, Navier-Stokes equations

Abstract

The numerical simulation of an incompressible and isothermal flow past a semi-infinite flat plate using the Navier-Stokes equations reveals an overshoot of the velocity not described in the literature. The main goal of this paper is to show that this overshoot is not a numerical artefact. A analytical study for both Stokes and Navier-Stokes equations allowed us to prove that this effect is not due to the inertial term but to the discontinuity of the boundary condition. We also carried out a detailed analysis of the transition zone for all values of viscosity. For small values, we retrieve a flow and a boundary layer similar to those predicted by Prandtl's theory, except near the origin of the plate.

1. Introduction

We are interested in the incompressible, isothermal two-dimensional viscous flow past a horizontal flat plate. This type of flow leads to the boundary layer theory Prandtl (1905, 1928), Blasius (1908, 1950), van Kármán (1921).

The flow takes place in the quarter plane $\mathbb{R}_+ \times \mathbb{R}_+$, and the system is governed by the Navier-Stokes equations and satisfies a homogeneous Dirichlet boundary condition along the plate $y = 0$ and a constant velocity $\boldsymbol{u} = (1, 0)$ on the inflow boundary $x = 0$.

When numerically solving this system by means of a finite element method in a bounded domain, we get an overshoot for the component of the velocity which is parallel to the plate. This phenomenon, which cannot occur in the boundary layer theory, has been noted in the literature at several places Gatski & Grosch (1987), Dijkstra & Kuerten (1993), (Çengel & Cimbala 2006, pp. 546-547). According to Gatski and Grosch, "[The figure] clearly shows a velocity overshoot of the order of 5 percent followed by a relaxation to the free-stream value. These results [...] indicate that in the region near the leading edge any results for the mean flow variables derivable from boundary-layer theory should be used with caution".

The effect of surface heating is also known to induce a stream-wise acceleration in the boundary layer which exhibits an overshoot of velocity Tunney et al. (2015).

The question which arises naturally is whether this phenomenon is only a numerical artefact or is really contained in the Navier-Stokes equations. The few authors who mention this overshoot usually associate it with *inertia* (Çengel & Cimbala 2006, pp. 546-547).

We show in this paper that the overshoot is actually inherent to the Stokes equations, and therefore is also present in the Navier-Stokes equations for all values of viscosity. We show that it is due to the discontinuity of the Dirichlet condition at the origin $(0, 0)$. For this purpose, we use a twofold approach: analytical, in the quarter plane, and numerical, in a bounded domain.

In order to obtain analytical expressions of the solutions, we rewrite the equations in terms of the vorticity ω and the stream function ϕ, in polar coordinates (r, θ). The idea is to develop (ϕ, ω) as power series with respect to r, which allows to study the behaviour of the solutions around the origin Evans et al. (1999), Burda et al. (2012). The first term of the Navier-Stokes expansion is the Stokes solution, whereas the following terms can be determined recursively.

We use the analytical expressions to highlight the presence of the velocity overshoot, in particular its amplitude and position.

Then we show that the analytical solution does not satisfy the conditions resulting from Prandtl's hypotheses, even for small values of the viscosity. In particular, the behaviour of the pressure is completely different from the one expected in the boundary layer theory, where the pressure is independent of y. The existence of the velocity overshoot leads us to propose a new definition of the boundary layer thickness δ.

Finally, we present numerical experiments, obtained by using a home-made library devoted to the finite element approximation of various problems in fluid mechanics. The numerical tests show that for small values of the viscosity and for x sufficiently large, the computed thickness is similar to the one given by Prandtl. However, near the origin, both our analytical and numerical results show that δ cannot behave as $\sqrt{x}$ since $\delta'(0) \neq \infty$, independently of the kinematic viscosity ν; the differences increase with the viscosity. The analytical and numerical solutions invalidate some of Prandtl's hypotheses, in particular near the origin of the plate which is neglected in the boundary layer theory.

2. Analytical approach for Stokes and Navier-Stokes equations

The model problem is governed by the incompressible Navier-Stokes equations in the quarter plane $\mathbb{R}_+ \times \mathbb{R}_+$:

$$\boldsymbol{u}\cdot\boldsymbol{\nabla}\boldsymbol{u} - \nu\Delta\boldsymbol{u} + \boldsymbol{\nabla}p = \boldsymbol{0}, \qquad \boldsymbol{\nabla}\cdot\boldsymbol{u} = 0, \tag{1.}$$

with ν the kinematic viscosity and p the normalized pressure.

We will also consider the Stokes equations:

$$-\nu\Delta\boldsymbol{u} + \boldsymbol{\nabla}p = \boldsymbol{0}, \qquad \boldsymbol{\nabla}\cdot\boldsymbol{u} = 0. \tag{2.}$$

On the lower boundary $y = 0$, representing a infinite flat plate, a wall boundary condition is satisfied, whereas on the inflow boundary $x = 0$ a flat velocity profile $(u_x^\infty, 0)$ is imposed. Without any loss of generality, we take $u_x^\infty = 1$.

For this flow configuration, and for the Stokes equations, the velocity profile is independent of the viscosity.

2.1. Vorticity-stream function formulation

The goal of this subsection is to write both Stokes and Navier-Stokes equations in terms of the vorticity and the stream function, and then to propose expansions of the solutions around the origin, by using polar coordinates.

For this purpose, we introduce the vorticity ω and the stream function ϕ as follows:

$$\omega = curl\,\boldsymbol{u} = \frac{\partial u_y}{\partial x} - \frac{\partial u_x}{\partial y}, \qquad \boldsymbol{u} = \mathrm{curl}\phi = (\frac{\partial\phi}{\partial y}, -\frac{\partial\phi}{\partial x}). \tag{3.}$$

The existence of ϕ is given by the incompressibility constraint; its uniqueness holds up to a constant. It is well-known that:

$$\omega = curl(\mathrm{curl}\phi) = -\Delta\phi. \tag{4.}$$

By applying the *curl* operator to the momentum conservation laws, we respectively get

$$-\nu\Delta\omega = 0 \tag{5.}$$

for the Stokes equations, and

$$-\nu\Delta\omega + \boldsymbol{\nabla}\omega\cdot\mathrm{curl}\phi = 0 \tag{6.}$$

for the Navier-Stokes equations. In the latter case, we have used that

$$\boldsymbol{u}\cdot\boldsymbol{\nabla}\boldsymbol{u} = \omega\boldsymbol{u}^\perp + \frac{1}{2}\boldsymbol{\nabla}(\boldsymbol{u}\cdot\boldsymbol{u}), \tag{7.}$$

with $\boldsymbol{u}^\perp = (-u_y, u_x) = \boldsymbol{\nabla}\phi$, such that $curl(\boldsymbol{u}\cdot\boldsymbol{\nabla}\boldsymbol{u}) = \boldsymbol{\nabla}\omega\cdot\mathrm{curl}\phi$.

The two systems (4)-(5) and (4)-(6) are closed by imposing the same boundary conditions: $\boldsymbol{u}(x,0) = (0,0)$, $\boldsymbol{u}(0,y) = (1,0)$.

To take into account the discontinuity of the velocity at the origin, we use polar coordinates (r,θ). Let us first recall the expression of some differential operators in polar coordinates:

$$\boldsymbol{\nabla}\phi = \frac{\partial\phi}{\partial r}\boldsymbol{e}_r + \frac{1}{r}\frac{\partial\phi}{\partial\theta}\boldsymbol{e}_\theta, \quad \mathrm{curl}\phi = \frac{1}{r}\frac{\partial\phi}{\partial\theta}\boldsymbol{e}_r - \frac{\partial\phi}{\partial r}\boldsymbol{e}_\theta, \quad \Delta\phi = \frac{\partial^2\phi}{\partial r^2} + \frac{1}{r}\frac{\partial\phi}{\partial r} + \frac{1}{r^2}\frac{\partial^2\phi}{\partial\theta^2}. \tag{8.}$$

By writing $\boldsymbol{u} = u_r \boldsymbol{e}_r + u_\theta \boldsymbol{e}_\theta$, we can next identify

$$u_r = \frac{1}{r}\frac{\partial \phi}{\partial \theta}, \qquad u_\theta = -\frac{\partial \phi}{\partial r}. \tag{9.}$$

Then the previous boundary conditions translate into:

$$\frac{\partial \phi}{\partial \theta}(r,0) = \frac{\partial \phi}{\partial \theta}\left(r, \frac{\pi}{2}\right) = 0, \quad \phi(r,0) = c_1, \quad \phi\left(r, \frac{\pi}{2}\right) = r + c_2. \tag{10.}$$

The continuity of ϕ as r tends to 0 yields $c_1 = c_2$, and since ϕ is unique up to a constant, we take $c_1 = 0$ in what follows.

To resume, solving the Stokes equations amounts to solving the following system of partial differential equations, independent of the viscosity ν:

$$\begin{cases} r^2 \dfrac{\partial^2 \omega}{\partial r^2} + r\dfrac{\partial \omega}{\partial r} + \dfrac{\partial^2 \omega}{\partial \theta^2} = 0, \\ r^2 \dfrac{\partial^2 \phi}{\partial r^2} + r\dfrac{\partial \phi}{\partial r} + \dfrac{\partial^2 \phi}{\partial \theta^2} = -r^2 \omega, \end{cases} \tag{11.}$$

together with the boundary conditions:

$$\phi(r,0) = 0, \quad \phi\left(r, \frac{\pi}{2}\right) = r, \quad \frac{\partial \phi}{\partial \theta}(r,0) = \frac{\partial \phi}{\partial \theta}\left(r, \frac{\pi}{2}\right) = 0. \tag{12.}$$

As regards the Navier-Stokes equations, they can be rewritten as follows:

$$\begin{cases} -\nu\left(r^2 \dfrac{\partial^2 \omega}{\partial r^2} + r\dfrac{\partial \omega}{\partial r} + \dfrac{\partial^2 \omega}{\partial \theta^2}\right) + r\left(\dfrac{\partial \omega}{\partial r}\dfrac{\partial \phi}{\partial \theta} - \dfrac{\partial \omega}{\partial \theta}\dfrac{\partial \phi}{\partial r}\right) = 0, \\ r^2 \dfrac{\partial^2 \phi}{\partial r^2} + r\dfrac{\partial \phi}{\partial r} + \dfrac{\partial^2 \phi}{\partial \theta^2} = -r^2 \omega, \end{cases} \tag{13.}$$

together with the same set of boundary conditions (12).

We agree to denote by (ϕ^S, ω^S) and (ϕ^{NS}, ω^{NS}) the Stokes and Navier-Stokes solutions, respectively.

In what follows, we look for ϕ^S as

$$\phi^S(r,\theta) = \sum_{n\in\mathbb{Z}} r^n \phi_n(\theta). \tag{14.}$$

Since ϕ^S is continuous as r tends to 0, we take $n \geq 0$. Moreover, one has

$$\begin{aligned} r^2 \Delta \phi^S &= r^2 \sum_{n\geq 2} n(n-1) r^{n-2} \phi_n + r \sum_{n\geq 1} n r^{n-1} \phi_n + \sum_{n\geq 0} r^n \phi_n'' \\ &= \sum_{n\in\mathbb{N}} \left(n^2 \phi_n + \phi_n''\right) r^n \end{aligned} \tag{15.}$$

which implies a similar expansion for ω^S:

$$\omega^S(r,\theta) = \sum_{n\in\mathbb{N}} r^{n-2} \omega_{n-2}(\theta). \tag{16.}$$

Exactly as for the Stokes equations, in the Navier-Stokes case we look for

$$\phi^{NS}(r,\theta) = \sum_{n\in\mathbb{N}} r^n \tilde{\phi}_n(\theta), \qquad \omega^{NS}(r,\theta) = \sum_{n\in\mathbb{N}} r^{n-2} \tilde{\omega}_{n-2}(\theta), \tag{17.}$$

where $\tilde{\phi}_n$ and $\tilde{\omega}_n$ now also depend on the viscosity ν.

2.2. Stokes equations in the quarter plane

Here, we only consider the Stokes equations in the quarter plane and we solve the system of partial differential equations (11)-(12).

Thanks to the expansions (14) and (16), we have to solve for any $n \in \mathbb{N}$ the decoupled ordinary differential equations:

$$\begin{cases} \omega_{n-2}'' + (n-2)^2 \omega_{n-2} = 0 \\ \qquad\qquad \phi_n'' + n^2 \phi_n = -\omega_{n-2}, \end{cases} \tag{18.}$$

together with the boundary conditions:

$$\begin{cases} \quad \phi_n(0) = \phi_n\left(\dfrac{\pi}{2}\right) = 0, \quad n \in \mathbb{N} \setminus 1, \\ \phi_1(0) = 0, \quad \phi_1\left(\dfrac{\pi}{2}\right) = 1, \\ \quad \phi_n'(0) = \phi_n'\left(\dfrac{\pi}{2}\right) = 0, \quad n \in \mathbb{N}. \end{cases} \tag{19.}$$

We show in Appendix A that $\phi_n = \omega_{n-2} = 0$ for any $n \neq 1$, and we also calculate ϕ_1 and ω_{-1}. The exact Stokes solution in the quarter plane is finally given by:

$$\begin{cases} \phi^S(r,\theta) = r\phi_1(\theta) = \dfrac{2r\left(-2\sin\theta + 2\theta\cos\theta + \pi\theta\sin\theta\right)}{\pi^2 - 4}, \\ \omega^S(r,\theta) = \dfrac{1}{r}\omega_{-1}(\theta) = \dfrac{4(2\sin\theta - \pi\cos\theta)}{r(\pi^2-4)}. \end{cases} \tag{20.}$$

2.3. Navier-Stokes equations in the quarter plane

In this subsection, we consider the system of partial differential equations (13)-(12) and the expansions (17) for its solution. We have:

$$\begin{aligned} r^2 \Delta \omega^{NS} &= r^2 \sum_{n\in\mathbb{N}} (n-2)(n-3) r^{n-4} \tilde{\omega}_{n-2} + r \sum_{n\in\mathbb{N}} (n-2) r^{n-3} \tilde{\omega}_{n-2} + \sum_{n\in\mathbb{N}} r^{n-2} \tilde{\omega}_{n-2}'' \\ &= \sum_{n\in\mathbb{N}} \left((n-2)^2 \tilde{\omega}_{n-2} + \tilde{\omega}_{n-2}''\right) r^{n-2}. \end{aligned} \tag{21.}$$

To compute the non-linear term, it is useful to recall that

$$\left(\sum_{n\in\mathbb{N}} r^n a_n\right) \cdot \left(\sum_{n\in\mathbb{N}} r^n b_n\right) = \sum_{n\in\mathbb{N}} r^n c_n, \qquad c_n := \sum_{k=0}^{n} a_k b_{n-k}. \tag{22.}$$

Then

$$\begin{aligned} r^2 \boldsymbol{\nabla} \omega^{NS} \cdot \mathrm{curl} \phi^{NS} = \frac{1}{r^2} &\left(\sum_{n\in\mathbb{N}} r^n (n-2) \tilde{\omega}_{n-2}\right) \cdot \left(\sum_{n\in\mathbb{N}} r^n \tilde{\phi}_n'\right) \\ &- \frac{1}{r^2} \left(\sum_{n\in\mathbb{N}} r^n n \tilde{\phi}_n\right) \cdot \left(\sum_{n\in\mathbb{N}} r^n \tilde{\omega}_{n-2}'\right), \end{aligned}$$

such that we have:

$$r^2 \boldsymbol{\nabla}\omega^{NS} \cdot \mathrm{curl}\phi^{NS} = \sum_{n\in\mathbb{N}} r^{n-2}\tilde{z}_n, \qquad \tilde{z}_n = \sum_{k=0}^{n}(k-2)\tilde{\omega}_{k-2}\tilde{\phi}'_{n-k} - k\tilde{\phi}_k\tilde{\omega}'_{n-k-2}. \quad 23.$$

Thus, we have to solve, for $n \in \mathbb{N}$:

$$\begin{cases} \nu\left((n-2)^2\tilde{\omega}_{n-2} + \tilde{\omega}''_{n-2}\right) = \tilde{z}_n, \\ n^2\tilde{\phi}_n + \tilde{\phi}''_n = -\tilde{\omega}_{n-2} \end{cases} \quad 24.$$

together with the same boundary conditions (12) as for the Stokes equations.

An important feature is that the previous system can be solved recurrently.

Indeed, for $n = 0$ the right-hand-side $\tilde{z}_0$ of the first equation is null so we can compute $\tilde{\omega}_{-2}$, and then $\tilde{\phi}_0$ from the second equation. It is important to note that the boundary conditions yield $\tilde{\phi}_0 = \tilde{\omega}_{-2} = 0$.

Next, for $n = 1$ we get $\tilde{z}_1 = 0$ and we retrieve exactly the same system as for the Stokes equations. So, the first terms in both the developments of ω^{NS} and ϕ^{NS} coincide with the Stokes solution.

Furthermore, for $n \geq 2$ we have:

$$\begin{aligned} \tilde{z}_n &= \sum_{k=1}^{n-1}(k-2)\tilde{\omega}_{k-2}\tilde{\phi}'_{n-k} - k\tilde{\phi}_k\tilde{\omega}'_{n-k-2} \\ &= \sum_{k=0}^{n-2}(k-1)\tilde{\omega}_{k-1}\tilde{\phi}'_{n-1-k} - (k+1)\tilde{\phi}_{k+1}\tilde{\omega}'_{n-k-3}. \end{aligned} \quad 25.$$

At the step n, one has already computed $\tilde{\omega}_i$ with $-2 \leq i \leq n-3$ and $\tilde{\phi}_j$ with $0 \leq j \leq n-1$, such that $\tilde{z}_n$ is known. Thus, one can find $\tilde{\omega}_{n-2}$ and then $\tilde{\phi}_n$ by solving a decoupled system of linear second-order differential equations.

Moreover, we can also deduce the dependence of $\tilde{\omega}_n$ and $\tilde{\phi}_n$ on the viscosity ν. We can easily check by recurrence that

$$\tilde{\omega}_{n-2} = \left(\frac{1}{\nu}\right)^{n-1}\omega_{n-2}(\theta), \quad \tilde{\phi}_n = \left(\frac{1}{\nu}\right)^{n-1}\phi_n(\theta), \quad n \geq 1. \quad 26.$$

Thus, we have obtained so far that:

$$\begin{aligned} \phi^{NS} &= \quad \nu\sum_{n=1}^{+\infty}\left(\frac{r}{\nu}\right)^n\phi_n = \phi^S + \nu\sum_{n=2}^{+\infty}\left(\frac{r}{\nu}\right)^n\phi_n, \\ \omega^{NS} &= \frac{1}{\nu}\sum_{n=-1}^{+\infty}\left(\frac{r}{\nu}\right)^n\omega_n = \omega^S + \frac{1}{\nu}\sum_{n=0}^{+\infty}\left(\frac{r}{\nu}\right)^n\omega_n, \end{aligned} \quad 27.$$

where

$$\phi^S = r\phi_1(\theta), \qquad \omega^S = \frac{1}{r}\omega_{-1}(\theta). \quad 28.$$

In Appendix B, we give the next two terms in the developments, (ϕ_2, ω_0) and (ϕ_3, ω_1), computed by using the free software MAXIMA; of course, one can compute more terms.

In Appendix C, we study from a numerical point of view the convergence of the expansions 27..

3. Velocity overshoot

3.1. Stokes equations

Using (9), we have that:

$$u_x^S(r,\theta) = u_r^S \cos\theta - u_\theta^S \sin\theta = \frac{1}{r}\frac{\partial \phi^S}{\partial \theta}\cos\theta + \frac{\partial \phi^S}{\partial r}\sin\theta, \tag{29.}$$

such that a simple computation gives:

$$u_x^S(\theta) = \phi_1'(\theta)\cos\theta + \phi_1(\theta)\sin\theta = \frac{2}{\pi^2-4}\left(\frac{\pi}{2}\sin 2\theta + \cos 2\theta + \pi\theta - 1\right). \tag{30.}$$

Noting that

$$(u_x^S)'(\theta) = \left(\phi_1''(\theta) + \phi_1(\theta)\right)\cos\theta = -\omega_{-1}(\theta)\cos\theta, \tag{31.}$$

one immediately obtains that the solutions of $(u_x^S)'(\theta) = 0$ are $\theta_S = \arctan\left(\frac{\pi}{2}\right)$ and $\frac{\pi}{2}$, which leads to:

$$\max_{0\le\theta\le\frac{\pi}{2}} u_x^S(\theta) = u_x^S(\theta_S) = \frac{2\pi}{\pi^2-4} > 1,\ u_x^S(\theta_S) = 1.07046\ldots. \tag{32.}$$

One can thus conclude that on the one hand, the velocity parallel to the plate is independent of r and its maximum is strictly larger than 1. On the other hand, the maxima at constant r are situated on the straight line $y = \frac{\pi}{2}x$, of polar angle θ_S.

3.2. Navier-Stokes equations

Similarly to (29), we have that

$$u_x^{NS}(r,\theta) = \frac{1}{r}\frac{\partial \phi^{NS}}{\partial \theta}\cos\theta + \frac{\partial \phi^{NS}}{\partial r}\sin\theta, \tag{33.}$$

with

$$\frac{\partial \phi^{NS}}{\partial r} = \sum_{n=1}^{+\infty} n\left(\frac{r}{\nu}\right)^{n-1}\phi_n, \quad \frac{\partial \phi^{NS}}{\partial \theta} = \nu\sum_{n=1}^{+\infty}\left(\frac{r}{\nu}\right)^n \phi_n'. \tag{34.}$$

This yields:

$$u_x^{NS}(r,\theta) = \sum_{n=1}^{+\infty}\left(\frac{r}{\nu}\right)^{n-1}\left(\phi_n'\cos\theta + n\phi_n\sin\theta\right) = u_x^S(\theta) + \sum_{n=1}^{+\infty}\left(\frac{r}{\nu}\right)^n \psi_n(\theta), \tag{35.}$$

with

$$\psi_n(\theta) = \phi_{n+1}'(\theta)\cos\theta + (n+1)\phi_{n+1}(\theta)\sin\theta. \tag{36.}$$

Thanks to the expression of ϕ_2 given in Appendix B, one can easily compute for $\theta_S = \arctan\frac{\pi}{2}$:

$$\psi_1(\theta_S) = \phi_2'(\theta_S)\cos\theta_S + 2\phi_2(\theta_S)\sin\theta_S = 0.020036\ldots > 0. \tag{37.}$$

Thus, for $\frac{r}{\nu}$ sufficiently small, we have that

$$u_x^{NS}(r,\theta_S) > u_x^S(\theta_S) > 1. \tag{38.}$$

Finally, we deduce that near the origin, as $r \to 0$, the maximum of the Navier-Stokes velocity parallel to the plate is superior to the maximum of the Stokes velocity, which is

larger than 1. For the Navier-Stokes equations, the value of the global maximum of u_x^{NS} depends on r too, which is not the case for the Stokes equations since $u_x^S = u_x^S(\theta)$.

To conclude, let us also consider the position of the maximum of u_x^{NS} at constant r, that is the polar angle $\theta_{NS}(r)$ such that

$$\frac{\partial u_x^{NS}}{\partial \theta}(r, \theta_{NS}(r)) = 0. \tag{39.}$$

By passing to the limit as $r \to 0$ in the equality $\frac{\partial u_x^{NS}}{\partial \theta} = \frac{\partial u_x^S}{\partial \theta} + \sum_{n=1}^{+\infty} \left(\frac{r}{\nu}\right)^n \psi_n'(\theta)$, we obtain that

$$0 = \lim_{r \to 0} \frac{\partial u_x^S}{\partial \theta}\left(\theta_{NS}\left(r\right)\right) = \frac{\partial u_x^S}{\partial \theta}\left(\lim_{r \to 0} \theta_{NS}\left(r\right)\right). \tag{40.}$$

Since $\frac{\partial u_x^S}{\partial \theta}$ vanishes only at θ_S, we deduce that $\lim_{r \to 0} \theta_{NS}(r) = \theta_S$.

So, the curve describing the position of the maximum of u_x at constant r is tangent at the origin to the Stokes straight line.

4. Prandtl's theory

In view of further comparison with our approach, we briefly recall the classical boundary layer theory of Prandtl.

For a flow past a flat plate of length L and in the case of an incompressible fluid with a small viscosity, a thin transition layer with great velocity gradient appears, called the boundary layer of thickness $\delta\left(x\right) \ll x$ with $0 < x \leq L$ Prandtl (1905, 1928).

The incompressibility condition leads to $\frac{u_x}{x} \sim \frac{u_y}{\delta\left(x\right)}$; it follows that $u_y \ll u_x$ and $\frac{\partial u_x}{\partial x} \ll \frac{\partial u_x}{\partial y}$.

Near the plate, the flow is governed by the viscosity effect $\nu \frac{\partial^2 u_x}{\partial y^2}$, whereas in the remainder of the fluid the inertial effect $u_x \frac{\partial u_x}{\partial x}$ is preponderant. The continuity between the boundary layer flow and the non-perturbated Euler flow implies that $u_x \frac{\partial u_x}{\partial x} \sim \nu \frac{\partial^2 u_x}{\partial y^2}$ which leads to $\frac{u_x^2}{x} \sim \nu \frac{u_x}{\delta\left(x\right)^2}$. Since u_x is equal to u_x^∞, we then obtain the following relationship for the thickness of the boundary layer: $\delta(x) \sim \sqrt{\frac{\nu x}{u_x^\infty}}$. This also implies for the pressure gradient that $\frac{\partial p}{\partial y} \simeq 0$.

In summary, we can consider the following assumptions:

$$\frac{\partial u_x}{\partial x} \ll \frac{\partial u_x}{\partial y}, \quad u_y \ll u_x \quad \text{and} \quad \frac{\partial p}{\partial y} \simeq 0. \tag{41.}$$

The idea of Prandtl Prandtl (1905, 1928) was to look for a change of variables allowing to solve the PDE in ϕ. He proposed to look for ϕ as below:

$$\phi(x, y) = \sqrt{u_x^\infty \nu x}\, f(\eta), \quad \text{with} \quad \eta = y\sqrt{\frac{u_x^\infty}{\nu x}}. \tag{42.}$$

Then the PDE in ϕ translates into the following ODE in f Falkner & Skan (1930):

$$f \frac{d^2 f}{d\eta^2} + 2 \frac{d^3 f}{d\eta^3} = 0, \tag{43.}$$

Noting that

$$u_x = \frac{\partial \phi}{\partial y} = u_x^\infty \frac{df}{d\eta}, \qquad u_y = -\frac{\partial \phi}{\partial x} = \frac{1}{2}\sqrt{\frac{u_x^\infty \nu}{x}}\left(\eta \frac{df}{d\eta} - f\right), \tag{44.}$$

one can reformulate the boundary conditions on $\boldsymbol{u}$ in terms of f as follows:

$$\frac{df}{d\eta}(0) = 0, \quad \lim_{\eta \to \infty} \frac{df}{d\eta}(\eta) = 1, \quad f(0) = 0. \tag{45.}$$

Note that the previous change of variables does not hold for $x = 0$, which explains why the origin of the plate is never considered in the boundary layer theory. The boundary condition on the inflow is only partially imposed as $\eta \to \infty$. Indeed, $\eta \to \infty$ is achieved as $x \to 0$ or as $y \to \infty$. In the first case, one can see that u_y is not imposed on the inflow boundary. In the second case, the resolution of the ODE (43) together with the expression (44) of u_y yield that the latter is proportional to $x^{-1/2}$. Thus, for a given value of x, u_y does not vanish, which does not correspond to the physical reality.

In the classical boundary layer approach, u_x is a increasing function from zero on the plate to u_x^∞. By definition, the thickness of the boundary layer δ is obtained when u_x is equal to 99% of u_x^∞, which corresponds to $\eta = 4.92$. Thus, according to the definition of η in (42), one gets

$$\delta(x) = 4.92\sqrt{\frac{\nu x}{u_x^\infty}}. \tag{46.}$$

One can furthermore relate the thickness of the boundary layer to the velocity gradient on the plate $\frac{\partial u_x}{\partial y}(x, 0)$. For this purpose, we derive the equality $u_x = u_x^\infty \frac{df}{d\eta}$ and we obtain:

$$\frac{\partial u_x}{\partial y}(x, y) = u_x^\infty f''(\eta)\sqrt{\frac{u_x^\infty}{\nu x}}, \tag{47.}$$

which next leads to

$$\delta(x) = \frac{4.92}{\frac{\partial u_x}{\partial y}(x, y)} u_x^\infty f''(\eta). \tag{48.}$$

By taking next $y = 0$ and by using that $f''(0) = 0.33206$, we finally obtain:

$$\delta(x) = \frac{1.63374}{\frac{\partial u_x}{\partial y}(x, 0)} u_x^\infty. \tag{49.}$$

5. Behaviour of the solutions near the origin

In order to study the behaviour of the solutions near the origin, we only use in this section the expansions of (ϕ^{NS}, ω^{NS}), which hold near the origin; we will also consider numerical results obtained in the whole domain Ω in subsection 6.2. For small viscosities and for the Navier-Stokes case, we compare the expressions of $\frac{\partial u_x}{\partial x}$, u_y and p with those given by Prandtl's theory.

5.1. Gradient of the velocity parallel to the plate u_x

We have

$$\frac{\partial u_x}{\partial x} = \frac{\partial u_x}{\partial r}\frac{\partial r}{\partial x} + \frac{\partial u_x}{\partial \theta}\frac{\partial \theta}{\partial x}, \qquad \frac{\partial u_x}{\partial y} = \frac{\partial u_x}{\partial r}\frac{\partial r}{\partial y} + \frac{\partial u_x}{\partial \theta}\frac{\partial \theta}{\partial y}, \tag{50.}$$

with

$$\frac{\partial r}{\partial x} = \cos\theta, \quad \frac{\partial \theta}{\partial x} = -\frac{\sin\theta}{r}, \quad \frac{\partial r}{\partial y} = \sin\theta, \quad \frac{\partial \theta}{\partial y} = \frac{\cos\theta}{r}. \tag{51.}$$

We recall that

$$u_x(r,\theta) = \frac{1}{r}\frac{\partial \phi}{\partial \theta}\cos\theta + \frac{\partial \phi}{\partial r}\sin\theta \tag{52.}$$

which yield:

$$\begin{cases} \dfrac{\partial u_x}{\partial r} = -\dfrac{1}{r^2}\dfrac{\partial \phi}{\partial \theta}\cos\theta + \dfrac{1}{r}\dfrac{\partial^2 \phi}{\partial r \partial \theta}\cos\theta + \dfrac{\partial^2 \phi}{\partial r^2}\sin\theta, \\ \dfrac{\partial u_x}{\partial \theta} = \dfrac{1}{r}\dfrac{\partial^2 \phi}{\partial \theta^2}\cos\theta - \dfrac{1}{r}\dfrac{\partial \phi}{\partial \theta}\sin\theta + \dfrac{\partial^2 \phi}{\partial \theta \partial r}\sin\theta + \dfrac{\partial \phi}{\partial r}\cos\theta. \end{cases} \tag{53.}$$

By replacing (51) and (53) in (50), we get:

$$\frac{\partial u_x}{\partial x} = \frac{\cos^2\theta - \sin^2\theta}{r}\left(\frac{\partial^2 \phi}{\partial r \partial \theta} - \frac{1}{r}\frac{\partial \phi}{\partial \theta}\right) + \cos\theta\sin\theta\left(\frac{\partial^2 \phi}{\partial r^2} - \frac{1}{r}\frac{\partial \phi}{\partial r} - \frac{1}{r^2}\frac{\partial^2 \phi}{\partial \theta^2}\right), \tag{54.}$$

as well as

$$\frac{\partial u_x}{\partial y} = \frac{2\sin\theta\cos\theta}{r}\left(\frac{\partial^2 \phi}{\partial r \partial \theta} - \frac{1}{r}\frac{\partial \phi}{\partial \theta}\right) + \sin^2\theta\frac{\partial^2 \phi}{\partial r^2} + \cos^2\theta\left(\frac{1}{r}\frac{\partial \phi}{\partial r} + \frac{1}{r^2}\frac{\partial^2 \phi}{\partial \theta^2}\right). \tag{55.}$$

Let us begin with the Stokes equations, where $\phi^S(r,\theta) = r\phi_1(\theta)$. Then clearly

$$\begin{aligned} &\frac{\partial^2 \phi^S}{\partial r \partial \theta} - \frac{1}{r}\frac{\partial \phi^S}{\partial \theta} = \phi_1' - \phi_1' = 0, \\ &\frac{\partial^2 \phi^S}{\partial r^2} = 0, \\ &\frac{1}{r}\frac{\partial \phi^S}{\partial r} + \frac{1}{r^2}\frac{\partial^2 \phi^S}{\partial \theta^2} = \frac{1}{r}\left(\phi_1 + \phi_1''\right) = -\frac{1}{r}\omega_{-1} = -\omega^S. \end{aligned} \tag{56.}$$

So

$$\begin{aligned} &\frac{\partial u_x^S}{\partial x}(r,\theta) = -\frac{\sin\theta\cos\theta}{r}\left(\phi_1 + \phi_1''\right) = \frac{4(2\sin\theta - \pi\cos\theta)\sin\theta\cos\theta}{r(\pi^2 - 4)}, \\ &\frac{\partial u_x^S}{\partial y}(r,\theta) = \frac{\cos^2\theta}{r}\left(\phi_1 + \phi_1''\right) = -\frac{4(2\sin\theta - \pi\cos\theta)\cos^2\theta}{r(\pi^2 - 4)}. \end{aligned} \tag{57.}$$

For the Navier-Stokes equations, the calculation of $\frac{\partial u_x^{NS}}{\partial x}$ and $\frac{\partial u_x^{NS}}{\partial y}$ is detailed in Appendix D. From (117) we obtain:

$$\begin{aligned} &\frac{\partial u_x^{NS}}{\partial x} = \frac{\partial u_x^S}{\partial x} + \frac{1}{\nu}\sum_{n=2}^{+\infty}\left(\frac{r}{\nu}\right)^{n-2}\left((n-1)\phi_n'\cos 2\theta + \left(n(n-2)\phi_n - \phi_n''\right)\frac{\sin 2\theta}{2}\right), \\ &\frac{\partial u_x^{NS}}{\partial y} = \frac{\partial u_x^S}{\partial y} + \frac{1}{\nu}\sum_{n=2}^{+\infty}\left(\frac{r}{\nu}\right)^{n-2}\left((n-1)\phi_n'\sin 2\theta + n(n-1)\phi_n\sin^2\theta + \left(n\phi_n + \phi_n''\right)\cos^2\theta\right). \end{aligned} \tag{58.}$$

We note that the blow-up behaviour as r tends to 0 of the Stokes terms $\frac{\partial u_x^S}{\partial x}$ and $\frac{\partial u_x^S}{\partial y}$ implies the blow-up of the Navier-Stokes ones. Indeed, the difference between the Navier-Stokes and the Stokes terms is bounded as r tends to 0.

Let us next compare $\frac{\partial u_x^{NS}}{\partial x}$ and $\frac{\partial u_x^{NS}}{\partial y}$, according to (41). Thanks to (57) and (58), we obtain that:

$$\lim_{r\to 0} \frac{\frac{\partial u_x^{NS}}{\partial x}}{\frac{\partial u_x^{NS}}{\partial y}} = \lim_{r\to 0} \frac{\frac{\partial u_x^{S}}{\partial x}}{\frac{\partial u_x^{S}}{\partial y}} = -\tan\theta. \tag{59.}$$

We recall that the ratio $(\frac{\partial u_x}{\partial x})/(\frac{\partial u_x}{\partial y})$ is supposed to be $\ll 1$ in the boundary layer theory. However, we see from (59) that near the origin, this quantity blows up as $\theta \to \frac{\pi}{2}$ for all values of viscosities. According to Prandtl's theory, the thickness of the boundary layer is given by $\delta(x) \simeq \sqrt{x}$, which has a vertical tangent at the origin, corresponding to $\theta \to \frac{\pi}{2}$. So this invalidates the hypothesis $\frac{\partial u_x}{\partial x} \ll \frac{\partial u_x}{\partial y}$.

5.2. Velocity perpendicular to the plate u_y

The velocity u_y is given by

$$u_y = \frac{1}{r}\frac{\partial \phi}{\partial \theta}\sin\theta - \frac{\partial \phi}{\partial r}\cos\theta. \tag{60.}$$

Thus, for the Stokes equations we get

$$u_y^S = \phi_1' \sin\theta - \phi_1 \cos\theta = \frac{2}{\pi^2 - 4}\left(\pi \sin^2\theta + \sin 2\theta - 2\theta\right), \tag{61.}$$

whereas for the Navier-Stokes equations we obtain, thanks to (34), that

$$u_y^{NS} = u_y^S + \sum_{n=1}^{+\infty} \left(\frac{r}{\nu}\right)^n \left(\phi_{n+1}' \sin\theta - (n+1)\phi_{n+1}\cos\theta\right). \tag{62.}$$

A simple computation gives:

$$\lim_{r\to 0} \frac{u_y^{NS}}{u_x^{NS}} = \frac{u_y^S(\theta)}{u_x^S(\theta)} \tag{63.}$$

Noting that $(u_y^S)'(\theta) = (\phi_1'' + \phi_1)\sin\theta = -\omega_{-1}\sin\theta$, one easily gets that

$$\left(\frac{u_y^S}{u_x^S}\right)'(\theta) = -\frac{\omega_{-1}(u_x^S \sin\theta - u_y^S\cos\theta)}{(u_x^S)^2} = -\frac{\omega_{-1}\phi_1}{(u_x^S)^2}. \tag{64.}$$

Further analysis shows that the maximum of the ratio u_y^S/u_x^S is attained for $\theta = \theta_S$ and is equal to $\frac{1}{\theta_S} - \frac{2}{\pi}$, so is not negligible.

5.3. Pressure p

We are now interested in the analytical expression of the pressure, for both the Stokes and the Navier-Stokes equations.

For the Stokes equations, we have thanks to the incompressibility condition that

$$\boldsymbol{\nabla} p^S = \nu \Delta \boldsymbol{u}^S = -\nu\, \mathrm{curl}\omega^{\mathrm{S}}. \tag{65.}$$

In polar coordinates, this gives:

$$\frac{\partial p^S}{\partial r} = -\frac{\nu}{r}\frac{\partial \omega^S}{\partial \theta} = -\frac{\nu}{r^2}\omega_{-1}'(\theta), \qquad \frac{1}{r}\frac{\partial p^S}{\partial \theta} = \nu\frac{\partial \omega^S}{\partial r} = -\frac{\nu}{r^2}\omega_{-1}(\theta). \tag{66.}$$

A simple integration, together with the constraint $\omega_{-1}'' + \omega_{-1} = 0$, yields

$$p^S = \frac{\nu}{r}\omega_{-1}'(\theta) + c = \frac{4\nu(2\cos\theta + \pi\sin\theta)}{r(\pi^2-4)} + c, \quad c \in \mathbb{R}, \tag{67.}$$

as well as

$$\frac{\partial p^S}{\partial y} = \sin\theta\frac{\partial p^S}{\partial r} + \frac{\cos\theta}{r}\frac{\partial p^S}{\partial \theta} = \frac{\nu}{r^2}(\omega_{-1}''\cos\theta - \omega_{-1}'\sin\theta). \tag{68.}$$

Let us next consider the Navier-Stokes equations. As usually with the vorticity-stream function formulation, we first compute the dynamic pressure, defined by

$$p_d^{NS} = p^{NS} + \frac{1}{2}\boldsymbol{u}^{NS}\cdot\boldsymbol{u}^{NS} \tag{69.}$$

and satisfying the equation:

$$\boldsymbol{\nabla} p_d^{NS} = -\nu\,\mathrm{curl}\omega^{\mathrm{NS}} - \omega^{\mathrm{NS}}\boldsymbol{\nabla}\phi^{\mathrm{NS}}. \tag{70.}$$

In polar coordinates, we have:

$$\frac{\partial p_d^{NS}}{\partial r} = -\frac{\nu}{r}\frac{\partial \omega^{NS}}{\partial\theta} + \omega^{NS}\frac{\partial\phi^{NS}}{\partial r}, \qquad \frac{1}{r}\frac{\partial p_d^{NS}}{\partial\theta} = \nu\frac{\partial\omega^{NS}}{\partial r} - \frac{\omega^{NS}}{r}\frac{\partial\phi^{NS}}{\partial\theta}. \tag{71.}$$

The details of the calculation of p_d^{NS} and p^{NS} are given in Appendix E. According to (128), we have:

$$p^{NS}(r,\theta) = p^S(r,\theta) - K\ln r - \sum_{n=1}^{+\infty}\left(\frac{r}{\nu}\right)^n\left(\frac{\omega_n' + A_n}{n} + \frac{C_n}{2}\right), \tag{72.}$$

where the constant K is given in (127) and A_n, C_n are defined in (119) and (124), respectively.

One can now compute $\frac{\partial p^{NS}}{\partial y}$:

$$\frac{\partial p^{NS}}{\partial y} = \sin\theta\frac{\partial p^{NS}}{\partial r} + \frac{\cos\theta}{r}\frac{\partial p^{NS}}{\partial\theta} = P_{reg} + P_{sing}, \tag{73.}$$

with P_{reg} a regular part, bounded with respect to r, and P_{sing} a singular part which blows up as r tend towards 0:

$$P_{sing} = \frac{\partial p^S}{\partial y} - \frac{K}{r}\sin\theta. \tag{74.}$$

This expression is contrary to Prandtl's theory, since the y-derivative of the Stokes and the Navier-Stokes pressure blows up as $r \to 0$.

6. Analytical and numerical results

6.1. Analytical Stokes solution

We begin by expressing the velocity field $\boldsymbol{u}^S$ and the pressure p^S in Cartesian coordinates. We immediately have from (30) and (61) that:

$$\begin{aligned} u_x^S(x,y) &= \frac{2}{\pi^2-4}\left(\pi\frac{xy}{x^2+y^2} - 2\frac{y^2}{x^2+y^2} + \pi\arctan\frac{y}{x}\right), \\ u_y^S(x,y) &= \frac{2}{\pi^2-4}\left(\pi\frac{y^2}{x^2+y^2} + 2\frac{xy}{x^2+y^2} - 2\arctan\frac{y}{x}\right). \end{aligned} \tag{75.}$$

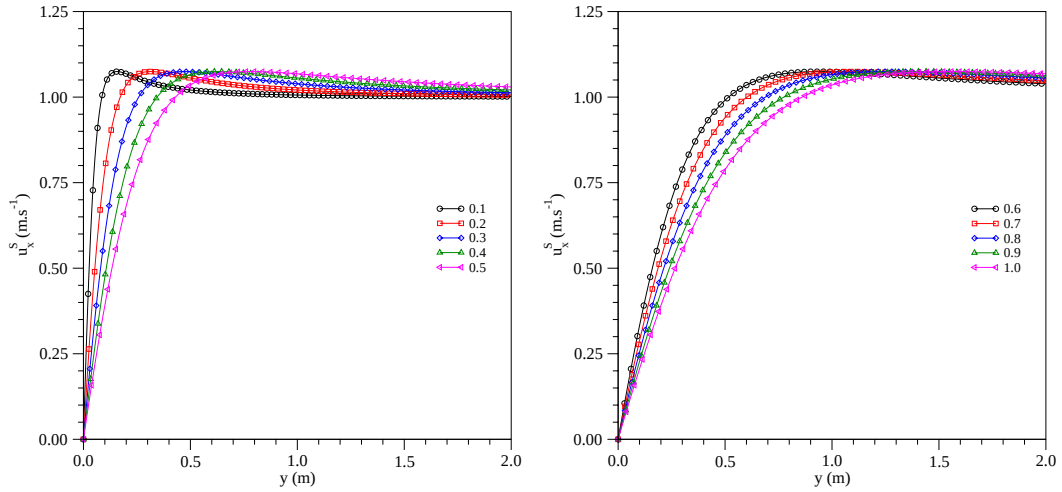

Figure 1

Stokes solutions. Profile of $u_x^S(x,\cdot)$: analytical results at different x.

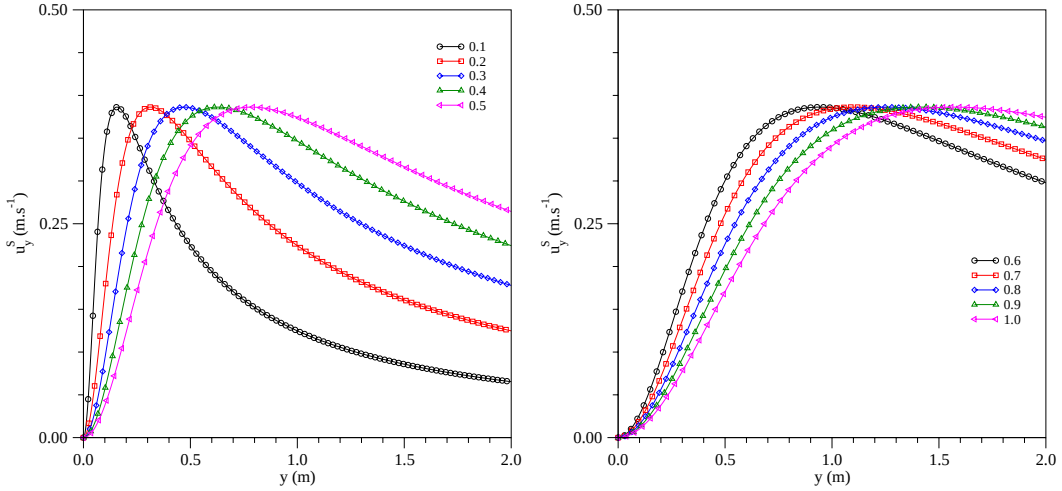

Figure 2

Stokes solutions. Profile of $u_y^S(x,\cdot)$: analytical results at different x.

The pressure is obtained from (67):

$$p^S(x,y) = \frac{4\nu(2x+\pi y)}{(\pi^2-4)(x^2+y^2)} + c, \quad c \in \mathbb{R}. \tag{76.}$$

The analytical values of the pressure are obtained by fixing a null pressure for $H = 3.2$ m and $L = 2.5$ m. We take 1 m^2.s^{-1} as the viscosity value to calculate the pressure. We thus

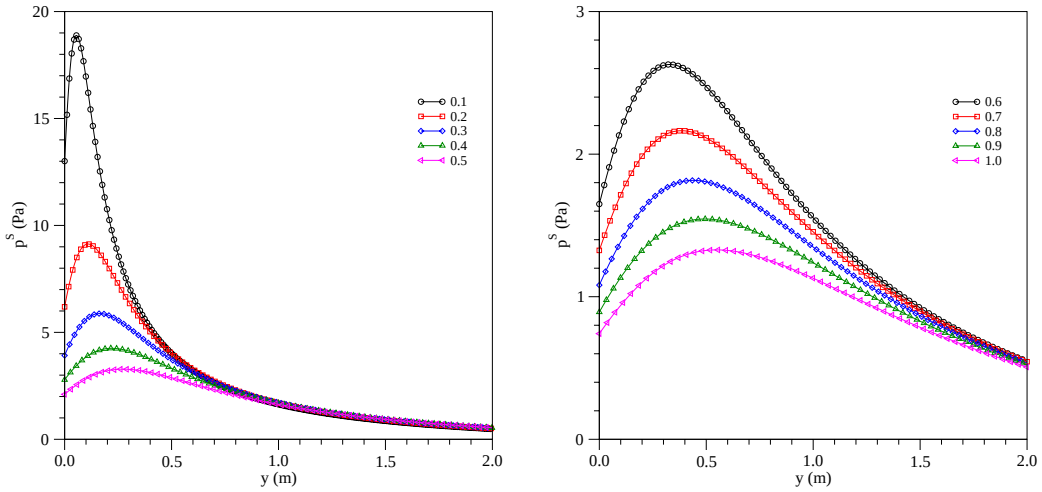

Figure 3

Stokes solutions. Profile of $p^S(x,\cdot)$: analytical results at different x.

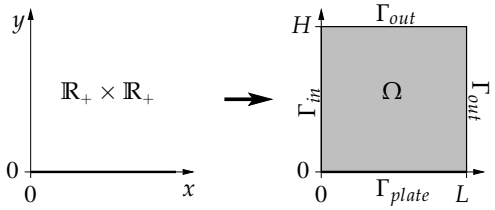

Figure 4

Original domain $(\mathbb{R}_+)^2$ and truncated domain Ω.

obtain:

$$p^S(x,y) = \frac{4\nu}{\pi^2 - 4}\left(\frac{2x+\pi y}{x^2+y^2} - \frac{2L+\pi H}{L^2+H^2}\right). \tag{77.}$$

In Fig. 1, Fig. 2 and Fig. 3, we represent the velocity field (u_x^S, u_y^S) given in (75) and the pressure p^S given in (77), for different abscissas x varying from 0.1 m to 1 m.

6.2. Analytical and numerical Navier-Stokes solution

Contrarily to the Stokes case, the analytical Navier-Stokes solution is written as a power series expansion in $\frac{r}{\nu}$, which limits the convergence domain as ν decreases. To overcome this problem, we solve the Navier-Stokes equations numerically, on a (sufficiently large) bounded domain $\Omega = [0, L] \times [0, H] \subset \mathbb{R}_+ \times \mathbb{R}_+$.

The system is closed by imposing an outflow condition on the artificial boundary Γ_{out} (see Fig. 4): $\nu(\nabla \boldsymbol{u})\boldsymbol{n} - p\boldsymbol{n} = \boldsymbol{0}$.

The numerical approximation is achieved by means of bilinear finite elements for both the velocity and the pressure, on quadrilateral meshes. A SUPG-type stabilization is em-

ployed in order to ensure the stability of the scheme. The boundary conditions are treated by using a Nitsche's approach; additional terms are introduced in the discrete formulation in order to control the discrete kinetic energy. This method has been developed and analyzed in Becker et al. (2015b,a). It has been validated numerically on different test-cases and for a large range of the viscosity parameter, by using a in-house C++ library, dedicated to fluid mechanics problems.

We next discuss the choice of the truncated computational domain Ω. It is well-known that the thickness of the boundary layer decreases with the viscosity, which implies to use a finer mesh near the plate as ν decreases. Therefore, in order to limit the number of cells, we chose to adapt the height H of the domain to the viscosity and to keep a constant length $L = 2.5$ m. Thus, for 10^{-3} m^2.s^{-1} $\leq \nu \leq 10$ m^2.s^{-1} we take $H = 3.2$ m, for 10^{-4} m^2.s^{-1} $\leq \nu \leq 10^{-3}$ m^2.s^{-1} we take $H = 1.8$ m and finally, for 10^{-5} m^2.s^{-1} $\leq \nu \leq 10^{-4}$ m^2.s^{-1} we impose $H = 0.8$ m. The solutions obtained for different meshes but the same values of the viscosity (10^{-3} and 10^{-4}) are in very good agreement. For all the tests, the number of cells is equal to 162180.

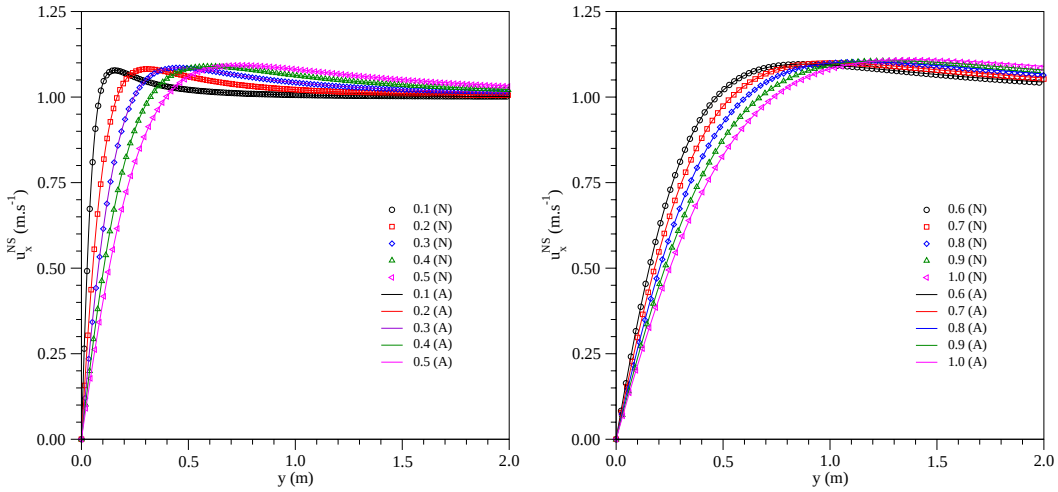

Figure 5

Navier-Stokes solutions. Profile of $u_x^{NS}(x, \cdot)$: analytical (A) and numerical (N) results at different x and for $\nu = 1$ m^2.s^{-1}.

We first validate the numerical results by comparison with the analytical ones, for a large value of the viscosity ($\nu = 1$ m^2.s^{-1}). As regards the analytical Navier-Stokes solution, we

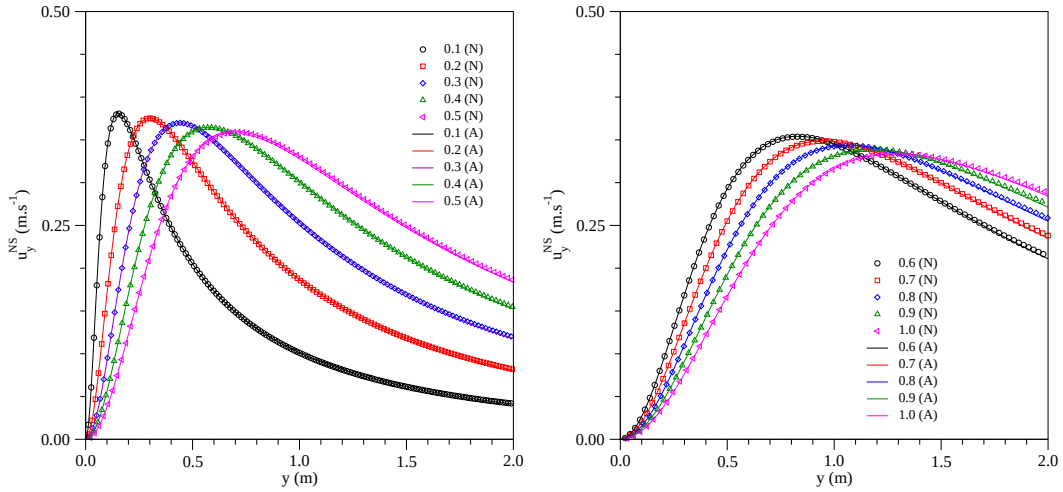

Figure 6

Navier-Stokes solutions. Profile of $u_y^{NS}(x,\cdot)$: analytical (A) and numerical (N) results at different x and for $\nu = 1$ m^2.s^{-1}.

consider only the first three terms in the expansions 35., 62. and 72.:

$$\tilde{u}_x^{NS} = u_x^S + \sum_{n=1}^{3} \left(\frac{r}{\nu}\right)^n \left(\phi'_{n+1}\cos\theta + (n+1)\,\phi_{n+1}\sin\theta\right), \tag{78.}$$

$$\tilde{u}_y^{NS} = u_y^S + \sum_{n=1}^{3} \left(\frac{r}{\nu}\right)^n \left(\phi'_{n+1}\sin\theta - (n+1)\phi_{n+1}\cos\theta\right), \tag{79.}$$

$$\tilde{p}^{NS} = p^S - K\ln r - \sum_{n=1}^{3} \left(\frac{r}{\nu}\right)^n \left(\frac{\omega'_n + A_n}{n} + \frac{C_n}{2}\right). \tag{80.}$$

As shown in Appendix C, the first three terms yield a sufficient accuracy in the case $\nu = 1$ m^2.s^{-1}.

The comparisons between the numerical results and $\tilde{u}_x^{NS}$, $\tilde{u}_y^{NS}$, $\tilde{p}^{NS}$, for different abscissas x varying from 0.1 m to 1 m, are presented in Fig. 5, Fig. 6 and Fig. 7. One can note on the one hand, the very good accuracy of the finite element method and on the other hand, the overshoot of u_x^{NS}.

We also observe an overshoot for the y component of the velocity, u_y^{NS}, Fig. 6 . This maximum is approximately 3 times lower than that obtained for u_x^{NS}.

The pressure presents a maximum near the plate which quickly descreases along the flow, Fig. 7. We note that the pressure does not vanish on the plate.

We next show in Fig. 8, Fig. 9 and Fig. 10 the computed Navier-Stokes solution, for a fixed abscissa $x = 0.5$ m and for different values of the viscosity ν, ranging from 10^{-5} to 1 m^2.s^{-1}. To determine the pressure in the Stokes case, we take $\nu = 1$ m^2.s^{-1}. We do not represent the Navier-Stokes curves for $\nu > 1$ m^2.s^{-1} since they are very close to the Stokes one.

The curves given in Fig. 8 and Fig. 9 show that the velocities overshoot are clearly

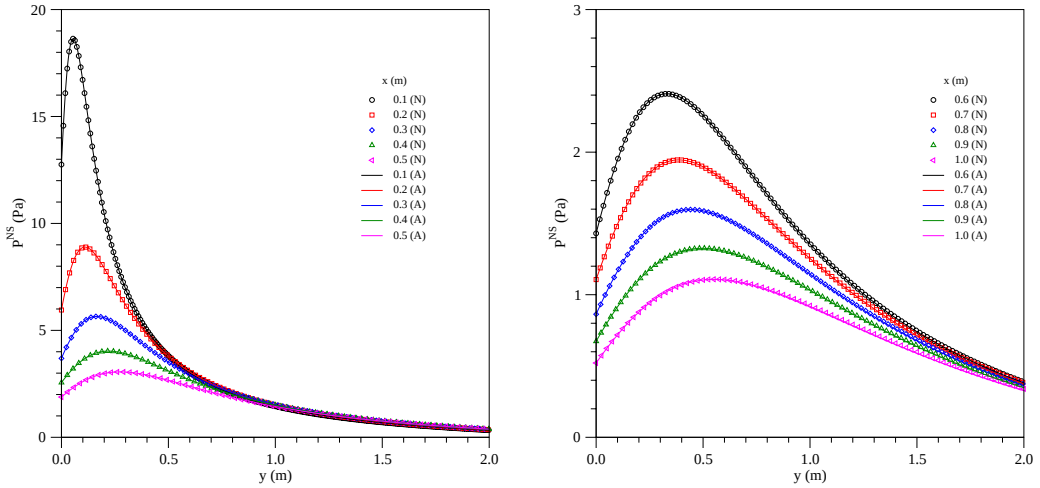

Figure 7

Navier-Stokes solutions. Profile of $p^{NS}(x,\cdot)$: analytical (A) and numerical (N) results at different x and for $\nu = 1$ m^2.s^{-1}.

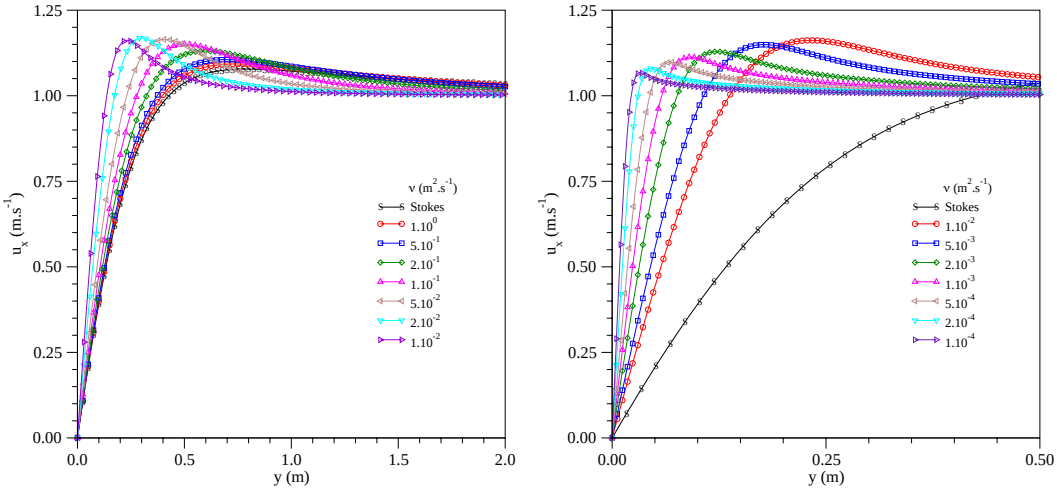

Figure 8

Navier-Stokes solutions. Profiles of computed $u_x(x,\cdot)$ at $x = 0.5$ m for different values of ν.

present for the whole range of viscosity. As expected, we observe that the position of the maximum gets closer to the plate as ν decreases. The thickness of the boundary layer defined by means of the component u_x decreases with the viscosity. As shown analytically in (38), we retrieve that the values of the u_x overshoot in the Navier-Stokes case are superior to that of the Stokes case. Moreover, for this given position, the values of the velocity overshoot

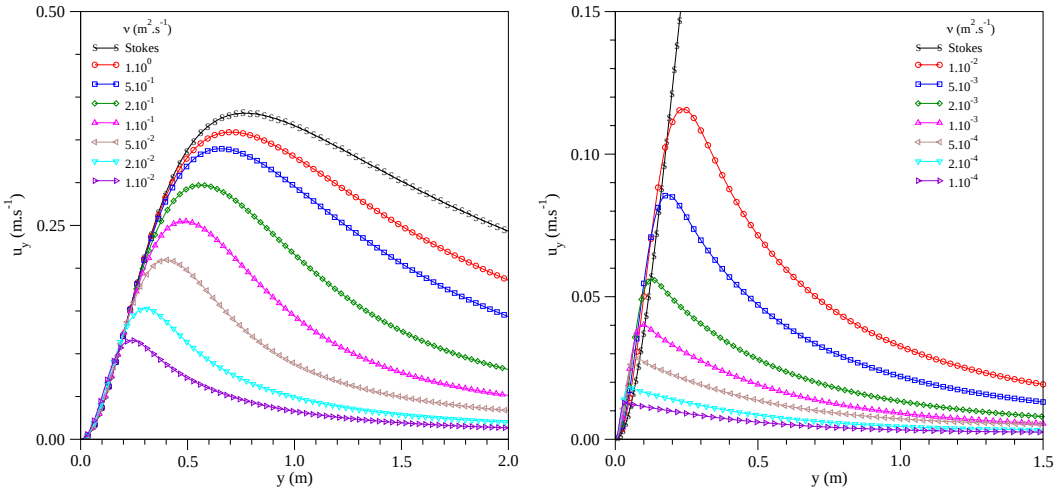

Figure 9

Navier-Stokes solutions. Profiles of computed $u_y(x,\cdot)$ at $x = 0.5$ m for different values of ν.

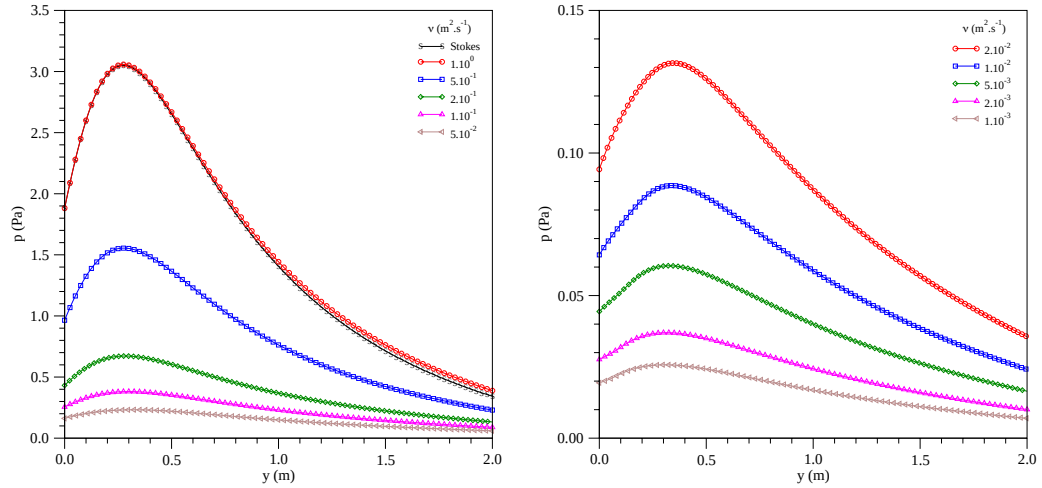

Figure 10

Navier-Stokes solutions. Profile of computed $p(x,\cdot)$ at $x = 0.5$ m for different values of ν.

decrease when the viscosity decreases. The component u_y tends to zero when y tends to infinity and decreases quickly with the viscosity.

In Fig. 11, we show $\boldsymbol{u}(x,y) = (u_x, u_y)$ given by the Falkner & Skan equations (44,43) and the numerical Navier-Stokes simulations for different values of viscosity, far from the origin at $x = 0.5$ m. The differential equation (43) was solved numerically.

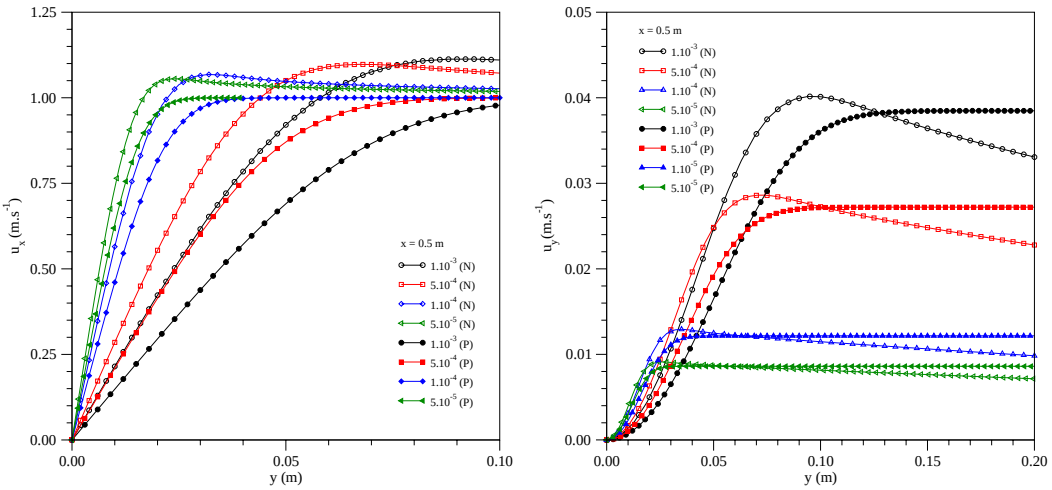

Figure 11

Navier-Stokes solutions. Profiles of $u_x^{NS}(x,\cdot)$ and $u_y^{NS}(x,\cdot)$: Prandtl's (P) and numerical (N) results at $x = 0.5$ m for different ν.

As expected, the velocities u_x and u_y obtained with the Falkner & Skan equations do not exhibit any overshoot.

Outside the validity domain of Prandtl's theory (i.e. for large values of viscosity), the slopes of the curves u_x near the plate are very different in the two approaches. However, when the viscosity decreases ($\nu < 10^{-5}$ m^2.s^{-1}), the velocity profiles are very close. For u_y, the two approaches yield a similar behaviour near the plate. The limit of u_y as $y \to \infty$ is not zero in Prandtl's approach, contrarily to ours.

As the velocities, the pressure presents an overshoot (Fig. 10). For this position $x = 0.5$ m, the pressure becomes negligible as the viscosity decreases. However, the pressure blows up at the origin and decreases in the direction of the flow for all values of viscosity (Fig. 12). In the Stokes case, the pressure along the plate is given by 67. with $\theta = 0$. This relationship clearly shows that the pressure diverges at the origin. We have the same behaviour for the analytical Navier-Stokes pressure, as can be seen in 72.. This behaviour is contrary to Prandtl's theory[1], where the pressure in the boundary layer is constant. Nevertheless, for a viscosity inferior to 10^{-5} m^2.s^{-1}, the pressure is negligible along the plate except near the origin, which is in agreement with Prandtl's assumption.

We end this section by a detailed analysis of the velocity overshoot. In Fig. 13, we present the position y of the velocity overshoot as a function of x, denoted by $\mathcal{C}_o$, for analytical Stokes solution and for the Navier-Stokes simulations, obtained for different viscosities.

As shown analytically in the Stokes case in subsection 3.1, the curve $\mathcal{C}_o^S$ is the straight line $y = \dfrac{\pi}{2}\, x$.

[1] "The lateral pressure differences can be disregarded, as likewise any curvature of the streamline. The pressure distribution will be impressed on the transition layer by the free fluid." Prandtl (1928)

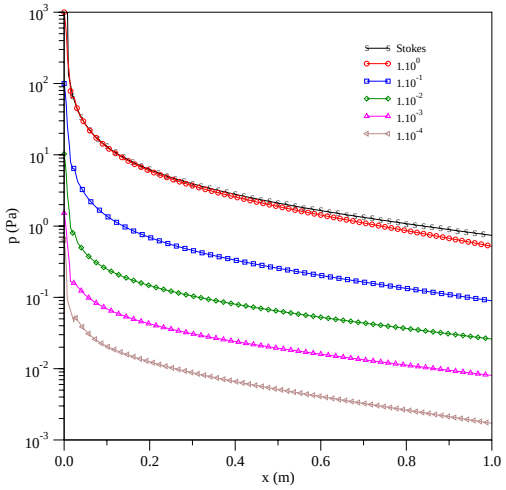

Figure 12

Profiles of $p(x,0)$: analytical Stokes pressure for $\nu = 1$ m^2.s^{-1} and numerical Navier-Stokes pressures for different ν.

ν (m^2.s^{-1})	Stokes	10^0	10^{-1}	10^{-2}	10^{-3}
u_{max} (m.s^{-1})	1.07046	1.11557	1.16490	1.16986	1.18774
Position (m)	—	1.635	1.490	0.205	0.015

Table 1 Value and position of the maximum velocity overshoot for different viscosities

For the Navier-Stokes case, all the curves $\mathcal{C}_o^{NS,\nu}$ are tangent to the Stokes one near the origin, as predicted by the analytical expansions.

We have shown in subsection 3.1 that the value of the Stokes overshoot is constant on the line $\mathcal{C}_o^S$. Meanwhile, in the Navier-Stokes case, the value of the overshoot on the curve $\mathcal{C}_o^{NS,\nu}$ presents a maximum. In Tab. 1, we give the value and the position x of this maximum for different viscosities. We note that these values are superior to the Stokes one and they increase when the viscosity decreases. As regards the positions, they tend to the origin of the plate when the viscosity decreases.

7. Boundary layer thickness

7.1. Definition and numerical results

Due to the existence of the overshoot, it seems delicate to define the thickness of the boundary layer in relation with a particular point of the curve u_x because several choices are possible. Therefore, we propose the following definition of the thickness:

$$\mathfrak{d}\,(x) = \frac{u_x^\infty}{\frac{\partial u_x}{\partial y}(x,0)}. \qquad 81.$$

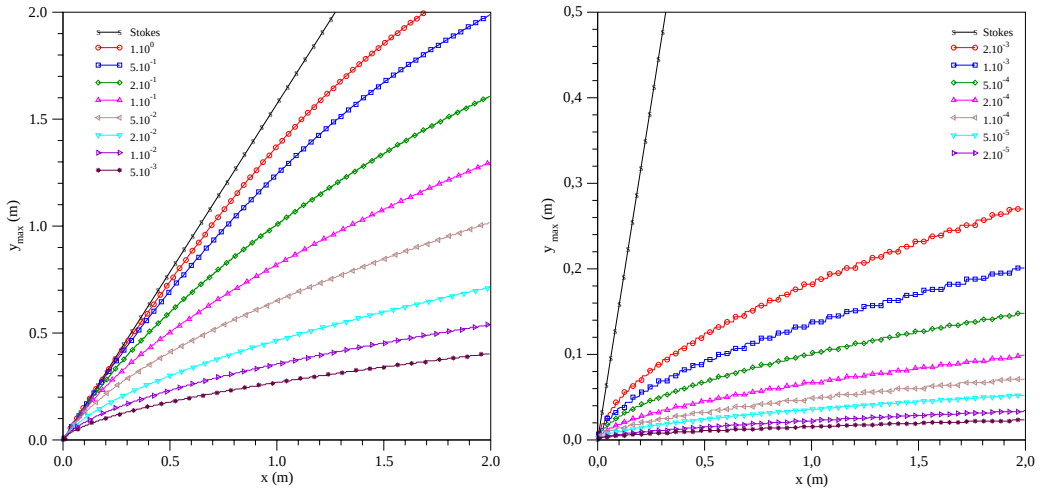

Figure 13

Position y of the velocity overshoot.

This definition is similar to Prandtl's relation (49). Our $\mathfrak{d}$ can be interpreted as the ordinate y where the first-order approximation of u_x near the origin is equal to u_x^∞.

As mentioned before, we take $u_x^\infty = 1$. By using the analytical expression of the velocity, we next compute $\mathfrak{d}(x)$ for both the Stokes and the Navier-Stokes equations. By taking $\theta = 0$ in (57) and in (58) and by using the boundary conditions $\phi_n(0) = \phi_n'(0) = 0$, we get

$$\frac{\partial u_x^S}{\partial y}(r,0) = \frac{1}{r}\phi_1''(0) = \frac{4\pi}{(\pi^2-4)r}, \qquad \frac{\partial u_x^{NS}}{\partial y}(r,0) = \frac{1}{r}\sum_{n=1}^{+\infty}\left(\frac{r}{\nu}\right)^{n-1}\phi_n''(0). \tag{82.}$$

In conclusion, since $r = x$ on the boundary $y = 0$, we have obtained so far that the thickness $\mathfrak{d}$ is linear (and independent of ν) in the Stokes case:

$$\mathfrak{d}^S(x) = \frac{1}{\frac{\partial u_x^S}{\partial y}(x,0)} = \frac{\pi^2-4}{4\pi}\,x. \tag{83.}$$

In the Navier-Stokes case, for $\frac{x}{\nu}$ sufficiently small, we have:

$$\mathfrak{d}^{NS}(x) = \frac{\mathfrak{d}^S(x)}{1 + a_1\frac{x}{\nu} + a_2\left(\frac{x}{\nu}\right)^2 + \cdots}, \tag{84.}$$

where

$$a_n = \frac{\phi_{n+1}''(0)}{\phi_1''(0)}, \qquad n \geq 1. \tag{85.}$$

It is important to note that

$$\left(\mathfrak{d}^{NS}\right)'(0) = \left(\mathfrak{d}^S\right)'(0) = \frac{\pi^2-4}{4\pi} = 0.467088\ldots \tag{86.}$$

This shows that our $\mathfrak{d}(x)$ does not behave as $\sqrt{x}$ near the origin, as proposed in the boundary layer theory, see 46..

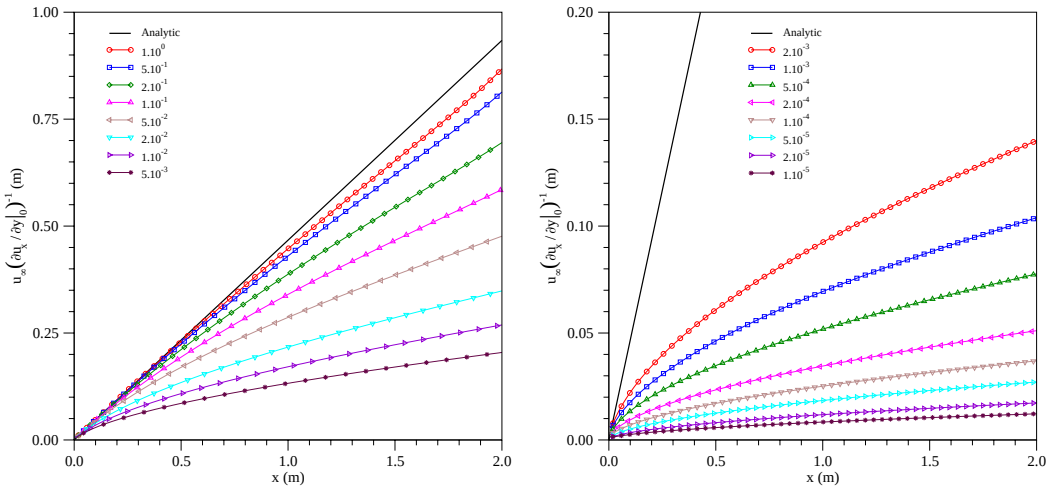

Figure 14

Boundary layer thickness $\mathfrak{d}(x)$ for different ν: numerical results.

Fig. 14 shows the variation of our boundary layer thickness (81) with respect to the viscosity, obtained by numerical simulations. We have also represented the analytical expression (83) for the Stokes equations. As regards the Navier-Stokes case, we numerically retrieve that the curves are tangent to the Stokes line near the origin, as given by (86). As expected, the thickness decreases with the viscosity.

7.2. Simplified formula of the thickness

The expansion (84) holds true for $\frac{x}{\nu}$ sufficiently small. Thus, the validity domain of a truncated expression of $\mathfrak{d}^{NS}$ decreases with ν. This limits the employ of such a truncated formula in order to fit the numerical results, for a large range of viscosity.

We propose the following analytical formula for the Navier-Stokes case:

$$\tilde{\mathfrak{d}}^{NS}(x) = \frac{\mathfrak{d}^{S}(x)}{1 + \alpha \left(\frac{x}{\nu}\right)^{\beta}} \tag{87.}$$

and we determine the coefficients α and β by least-squares fitting, see Fig. 15. In Tab. 2 we have given these regression coefficients, as well as the coefficient of determination R, for a whole range of viscosity values. Note that R is close to 1 for all ν.

Let us next focus on the exponent β, which varies from ≈ 1 to ≈ 0.5. The transition mainly takes place as ν varies from 1 $\mathrm{m}^2.\mathrm{s}^{-1}$ to 10^{-2} $\mathrm{m}^2.\mathrm{s}^{-1}$.

For $\nu \gtrsim 1$ $\mathrm{m}^2.\mathrm{s}^{-1}$, we obtain that $\beta \approx 1$ and $\alpha \approx a_1$, such that the fitting $\tilde{\mathfrak{d}}^{NS}$ is close to the first-order truncation of $\mathfrak{d}^{NS}$, that is

$$\tilde{\mathfrak{d}}^{NS}(x) \approx \frac{\mathfrak{d}^{S}(x)}{1 + a_1 \frac{x}{\nu}}. \tag{88.}$$

For $\nu \leq 10^{-2}$ $\mathrm{m}^2.\mathrm{s}^{-1}$, we observe that β is close to 0.5, such that for x sufficiently large

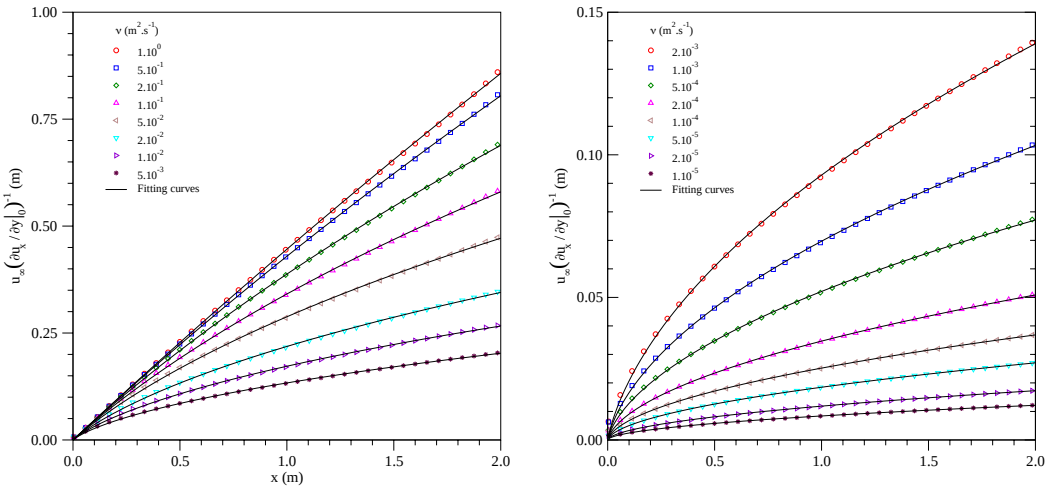

Figure 15

Boundary layer thickness for different ν: numerical results and fitting curves $\tilde{\mathfrak{d}}^{NS}$.

ν (m^2.s^{-1})	1.10^{1}	5.10^{0}	2.10^{0}	1.10^{0}	5.10^{-1}	2.10^{-1}	1.10^{-1}
α	0.157164	0.0937454	0.0568422	0.047572	0.047856	0.056545	0.069250
β	1.000000	1.000000	1.000000	0.922492	0.874493	0.799623	0.726510
R	0.999949	0.999959	0.999953	0.999961	0.999968	0.999963	0.999939
ν (m^2.s^{-1})	5.10^{-2}	2.10^{-2}	1.10^{-2}	5.10^{-3}	2.10^{-3}	1.10^{-3}	5.10^{-4}
α	0.086821	0.114184	0.135034	0.153834	0.173609	0.184575	0.208451
β	0.657249	0.587493	0.551382	0.526502	0.505996	0.496602	0.479370
R	0.999901	0.999859	0.999849	0.999852	0.999856	0.999839	0.999883
ν (m^2.s^{-1})	2.10^{-4}	1.10^{-4}	5.10^{-5}	2.10^{-5}	1.10^{-5}		
α	0.214288	0.223246	0.238193	0.245692	0.226348		
β	0.477176	0.473807	0.466875	0.466859	0.476344		
R	0.999876	0.999775	0.999954	0.999828	0.999422		

Table 2 Regression coefficients α and β for different values of viscosity.

we can write that

$$\tilde{\mathfrak{d}}^{NS}(x) \approx \frac{\mathfrak{d}^{S}(x)}{\alpha\sqrt{\frac{x}{\nu}}} = \gamma\sqrt{\nu x}, \qquad \gamma = \frac{\pi^2 - 4}{4\pi\alpha} \approx 1.868. \tag{89.}$$

In conclusion, for ν sufficiently small and x sufficiently large, Prandtl's approach and ours lead to the same description of the boundary layer thickness (up to a multiplicative factor). However, near the origin, the two approaches are different. In our case, as $\frac{x}{\nu}$ tends to 0, we retrieve the Stokes boundary layer thickness. In Prandtl's case, the tangent at the origin to the boundary layer is vertical.

8. Conclusions

The numerical simulation of an incompressible flow past a semi-infinite flat plate allowed us to exhibit the presence of a velocity overshoot. This phenomenon has already been noted in the literature without a convincing explanation. Thanks to a analytical study, we have been able to state that this overshoot is not a numerical artefact.

Moreover, we have shown that this phenomenon is not due to the inertial terms since it is already present in the Stokes equations. It is known that the Laplace operator does not yield such a behaviour (thanks to the maximum principle), therefore the overshoot is inherent to the Stokes operator combined with the discontinuity at the origin. In the Stokes case, the transition zone is delimited by a straight line independent of the viscosity.

As regards the Navier-Stokes equations, the presence of the inertial term modifies the transition zone, which now depends on the viscosity. We have noticed that when the viscosity decreases, the value of the overshoot increases and the position of the maximum gets closer to the plate. Thus for small viscosities, the transition zone can be assimilated to a boundary layer. The position of the maximum velocity overshoot gets closer to the origin of the plate as the viscosity decreases and the boundary layer is similar to the one proposed by Prandtl, except near the origin of the plate.

A. Calculation of the exact Stokes solution

We solve here the differential system (18)-(19).

We treat separately the cases $n = 0$ and $n - 2 = 0$. For $n = 0$, we obtain that $\omega_{-2} = A_{-2}\cos 2\theta + B_{-2}\sin 2\theta$ and $\phi_0 = C_0 + D_0\theta + E_0\cos 2\theta + F_0\sin 2\theta$, whereas for $n = 2$, we get $\omega_0 = A_0 + B_0\theta$ and $\phi_2 = C_2\cos 2\theta + D_2\sin 2\theta + E_2 + F_2\theta$. In both cases, the homogeneous boundary conditions immediately imply $\phi_0 = \phi_2 = 0$, and hence $\omega_{-2} = \omega_0 = 0$.

In the following, we consider $n \in \mathbb{N}\setminus\{0,2\}$. Then the first differential equation yields $\omega_{n-2} = A_{n-2}\cos(n-2)\theta + B_{n-2}\sin(n-2)\theta$ with A_{n-2}, $B_{n-2} \in \mathbb{R}$. In order to find a particular solution of the second differential equation, we have to distinguish whether $(n-2)^2$ is equal to n^2 or not, that is whether n is equal to 1 or not.

If $n \neq 1$, then

$$\phi_n = C_n\cos n\theta + D_n\sin n\theta + E_n\cos(n-2)\theta + F_n\sin(n-2)\theta. \tag{90.}$$

The homogeneous boundary conditions imply

$$E_n = -C_n, \qquad F_n = -\frac{n}{n-2}D_n \tag{91.}$$

as well as the linear system:

$$\begin{cases} \left(\cos\dfrac{n\pi}{2} - \cos\dfrac{(n-2)\pi}{2}\right)C_n + \left(\sin\dfrac{n\pi}{2} - \dfrac{n}{n-2}\sin\dfrac{(n-2)\pi}{2}\right)D_n = 0 \\ \left(-n\sin\dfrac{n\pi}{2} + (n-2)\sin\dfrac{(n-2)\pi}{2}\right)C_n + n\left(\cos\dfrac{n\pi}{2} - \cos\dfrac{(n-2)\pi}{2}\right)D_n = 0. \end{cases} \tag{92.}$$

Its discriminant Δ is equal to

$$\begin{aligned} \Delta &= 2n - 2n\cos\frac{n\pi}{2}\cos\frac{(n-2)\pi}{2} - \frac{n^2+(n-2)^2}{n-2}\sin\frac{n\pi}{2}\sin\frac{(n-2)\pi}{2} \\ &= 2n\left(1 - \cos\frac{n\pi}{2}\cos\frac{(n-2)\pi}{2} - \sin\frac{n\pi}{2}\sin\frac{(n-2)\pi}{2}\right) - \frac{4}{n-2}\sin\frac{n\pi}{2}\sin\frac{(n-2)\pi}{2} \\ &= 4n + \frac{2}{n-2}\Big(1+\cos(n-1)\pi\Big) = \frac{2}{n-2}\Big(1 + 2n(n-2) + \cos(n-1)\pi\Big). \end{aligned} \tag{93.}$$

Since $n \geq 3$ we have $\Delta \neq 0$. So we obtain $\phi_n = \omega_{n-2} = 0$ for $n \geq 3$.

Finally, let us consider the case $n = 1$. The previous approach leads to $\omega_{-1} = A_{-1}\cos\theta + B_{-1}\sin\theta$ but

$$\phi_1 = C_1\cos\theta + D_1\sin\theta + \theta(E_1\cos\theta + F_1\sin\theta). \tag{94.}$$

The boundary conditions now translate into:

$$C_1 = 0, \quad D_1 + F_1\frac{\pi}{2} = 1, \quad D_1 + E_1 = 0, \quad -C_1 - E_1\frac{\pi}{2} + F_1 = 0, \tag{95.}$$

which yield

$$C_1 = 0, \quad D_1 = -\frac{4}{\pi^2-4}, \quad E_1 = \frac{4}{\pi^2-4}, \quad F_1 = \frac{2\pi}{\pi^2-4}. \tag{96.}$$

This allows to obtain the only non-null terms in the Stokes expansions,

$$\phi_1(\theta) = \frac{2\left(-2\sin\theta + 2\theta\cos\theta + \pi\theta\sin\theta\right)}{\pi^2-4}, \qquad \omega_{-1}(\theta) = \frac{4(2\sin\theta - \pi\cos\theta)}{\pi^2-4}. \tag{97.}$$

B. Calculation of (ϕ_2, ω_0) and (ϕ_3, ω_1) in the Navier-Stokes expansion

For $n = 2$, the system to solve (24) is:

$$\begin{cases} \omega_0'' = -\omega_{-1}\phi_1' - \phi_1\omega_{-1}' = -(\omega_{-1}\phi_1)', \\ 4\phi_2 + \phi_2'' = -\omega_0. \end{cases} \tag{98.}$$

We obtain

$$\omega_0 = \frac{(8\pi\theta + \pi^2 - 12)\sin 2\theta + 8(2\theta + \pi)\cos 2\theta - 4(\pi^2 + 4)\theta\cos^2\theta + c_1 + c_2\theta}{(\pi^2 - 4)^2} \tag{99.}$$

and

$$\phi_2 = \frac{1}{(\pi^2 - 4)^2}\left(\frac{8(\pi^2 - 4)\theta^2 - 80\pi\theta - 3\pi^2 + 28}{32}\sin 2\theta + \frac{32\pi\theta^2 + (12\pi^2 - 112)\theta - 36\pi}{32}\cos 2\theta \right.$$
$$\left. + \frac{(-c_2 + 2\pi^2 + 8)\theta - c_1}{4} + k_1\sin 2\theta + k_2\cos 2\theta\right). \tag{100.}$$

By taking into account the boundary conditions (19), we obtain:

$$\phi_2 = \frac{1}{64(\pi^2 - 4)^2}\Big(\big(16(\pi^2 - 4)\theta^2 - 160\pi\theta - 2\pi^4 + 20\pi^2 + 112\big)\sin 2\theta$$
$$+ \big(64\pi\theta^2 + (24\pi^2 - 224)\theta + \pi(\pi^4 - 30\pi^2 + 56)\big)\cos 2\theta$$
$$+ 4\pi^2(\pi^2 - 16)\theta - \pi(\pi^4 - 30\pi^2 + 56)\Big), \tag{101.}$$

$$\omega_0 = \frac{1}{16(\pi^2 - 4)^2}\Big(16\left(8\pi\theta + \pi^2 - 12\right)\sin 2\theta + 32\left((4 - \pi^2)\theta + 4\pi\right)\cos 2\theta$$
$$+ 4\pi^2(16 - \pi^2)\theta + \pi(\pi^4 - 30\pi^2 + 56)\Big). \tag{102.}$$

For $n = 3$, we have to solve the system

$$\begin{cases} (\omega_1 + \omega_1'') = -\omega_{-1}\phi_2' - 2\omega_{-1}'\phi_2 - \omega_0'\phi_1, \\ 9\phi_3 + \phi_3'' = -\omega_1. \end{cases} \tag{103.}$$

Its solution is:

$$\phi_3 = \frac{1}{48^2(\pi^2 - 4)^3}\Big(P_3(\theta)\sin 3\theta + Q_3(\theta)\cos 3\theta + R_3(\theta)\sin\theta + S_3(\theta)\cos\theta\Big), \tag{104.}$$

$$\omega_1 = \frac{1}{24^2(\pi^2 - 4)^3}\Big(\tilde{P}_2(\theta)\sin 3\theta + \tilde{Q}_2(\theta)\cos 3\theta + \tilde{R}_3(\theta)\sin\theta + \tilde{S}_3(\theta)\cos\theta\Big), \tag{105.}$$

with:

$$P_3 = 96\pi(\pi^2-12)\theta^3 + 48(100-51\pi^2)\theta^2 + 8\pi(-3\pi^4+11\pi^2+1164)\theta \\ - 9\pi^6 + 487\pi^4 - 1608\pi^2 - 2320 \tag{106.}$$

$$Q_3 = 192(3\pi^2-4)\theta^3 + 24\pi(13\pi^2-252)\theta^2 + 2(3\pi^6-102\pi^4-1368\pi^2+4928)\theta \\ - 111\pi^5 + 1672\pi^3 + 336\pi \tag{107.}$$

$$R_3 = 192\pi(\pi^2+4)\theta^3 - 144(11\pi^2+12)\theta^2 - 72\pi(\pi^4-16\pi^2+8)\theta \\ + 3\pi^6 - 501\pi^4 + 4968\pi^2 - 2320 \tag{108.}$$

$$S_3 = 384(\pi^2+4)\theta^3 + 72\pi(3\pi^2-20)\theta^2 + 18(\pi^6-42\pi^4+144\pi^2-32)\theta \\ + 111\pi^5 - 1672\pi^3 - 336\pi \tag{109.}$$

$$\tilde{P}_2 = 864(3\pi^2-4)\theta^2 + 72\pi(11\pi^2-228)\theta + 9(\pi^6-34\pi^4-320\pi^2+1376) \tag{110.}$$

$$\tilde{Q}_2 = 432\pi(12-\pi^2)\theta^2 + 144(45\pi^2-92)\theta + 36\pi(\pi^4-8\pi^2-304) \tag{111.}$$

$$\tilde{R}_3 = -384\pi(\pi^2+4)\theta^3 + 288(13\pi^2+20)\theta^2 + 72\pi(2\pi^4-33\pi^2-20)\theta \\ + 3\pi^6 + 624\pi^4 - 7848\pi^2 + 5216 \tag{112.}$$

$$\tilde{S}_3 = -768(\pi^2+4)\theta^3 + 144\pi(12-5\pi^2)\theta^2 - 36(\pi^6-42\pi^4+116\pi^2-16)\theta \\ - 2\pi(93\pi^4-1330\pi^2-840). \tag{113.}$$

C. Convergence of the expansions

We are interested in the convergence of the expansions for $\omega, \phi, \dfrac{\partial\omega}{\partial\theta}$ and $\dfrac{\partial\phi}{\partial\theta}$, which ensure the convergence of all the other expansions in the paper. For a power expansion series $\sum_{n=0}^{\infty} a_n(\theta)\left(\dfrac{r}{\nu}\right)^n$, it is well-known that if $\|a_n\|_\infty = \max_\theta |a_n(\theta)|$ is bounded independently of n, then the convergence radius of the series is at least equal to ν.

In Fig. 16, we show that these norms are not only bounded but they quickly decrease as n increases. This leads us to believe that the convergence radius is certainly larger than ν.

D. Calculation of $\left(\frac{\partial u_x^{NS}}{\partial x}, \frac{\partial u_x^{NS}}{\partial y}\right)$

The first order derivatives of ϕ^{NS} are given in (34). As regards the second order derivatives, we have:

$$\frac{\partial^2\phi^{NS}}{\partial r\partial\theta} = \sum_{n=1}^{+\infty} n\left(\frac{r}{\nu}\right)^{n-1}\phi_n'(\theta),$$

$$\frac{\partial^2\phi^{NS}}{\partial r^2} = \sum_{n=1}^{+\infty} \frac{n(n-1)}{r}\left(\frac{r}{\nu}\right)^{n-1}\phi_n, \tag{114.}$$

$$\frac{\partial^2\phi^{NS}}{\partial\theta^2} = \sum_{n=1}^{+\infty} r\left(\frac{r}{\nu}\right)^{n-1}\phi_n''.$$

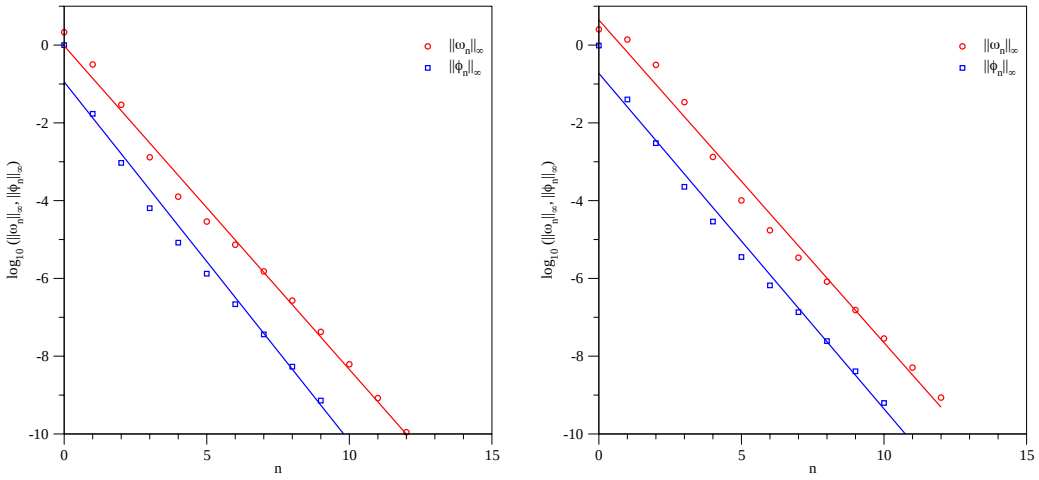

Figure 16

Maximum values of the coefficients $\omega_n, \phi_n, \omega_n'$ and ϕ_n' of the expansions.

In order to compute the gradient of u_x^{NS}, we use the expressions (54) and (55), which can be written as follows:

$$\begin{aligned}
\frac{\partial u_x^{NS}}{\partial x} &= \frac{\cos 2\theta}{r}\left(\frac{\partial^2\phi^{NS}}{\partial r\partial\theta} - \frac{1}{r}\frac{\partial\phi^{NS}}{\partial\theta}\right) + \frac{\sin 2\theta}{2}\left(\frac{\partial^2\phi^{NS}}{\partial r^2} - \frac{1}{r}\frac{\partial\phi^{NS}}{\partial r} - \frac{1}{r^2}\frac{\partial^2\phi^{NS}}{\partial\theta^2}\right),\\
\frac{\partial u_x^{NS}}{\partial y} &= \frac{\sin 2\theta}{r}\left(\frac{\partial^2\phi^{NS}}{\partial r\partial\theta} - \frac{1}{r}\frac{\partial\phi^{NS}}{\partial\theta}\right) + \sin^2\theta\frac{\partial^2\phi^{NS}}{\partial r^2} + \cos^2\theta\left(\frac{1}{r}\frac{\partial\phi^{NS}}{\partial r} + \frac{1}{r^2}\frac{\partial^2\phi}{\partial\theta^2}\right).
\end{aligned} \tag{115.}$$

We have

$$\begin{aligned}
\frac{\partial^2\phi^{NS}}{\partial r\partial\theta} - \frac{1}{r}\frac{\partial\phi^{NS}}{\partial\theta} &= \sum_{n=1}^{+\infty}(n-1)\left(\frac{r}{\nu}\right)^{n-1}\phi_n',\\
\frac{\partial^2\phi^{NS}}{\partial r^2} &= \frac{1}{r}\sum_{n=1}^{+\infty}\left(\frac{r}{\nu}\right)^{n-1} n(n-1)\phi_n,\\
\frac{1}{r}\frac{\partial\phi^{NS}}{\partial r} + \frac{1}{r^2}\frac{\partial^2\phi^{NS}}{\partial\theta^2} &= \frac{1}{r}\sum_{n=1}^{+\infty}\left(\frac{r}{\nu}\right)^{n-1}\left(n\phi_n + \phi_n''\right),
\end{aligned} \tag{116.}$$

so by replacing in (115), we obtain:

$$\begin{aligned}
\frac{\partial u_x^{NS}}{\partial x} &= \frac{1}{r}\sum_{n=1}^{+\infty}\left(\frac{r}{\nu}\right)^{n-1}\left((n-1)\phi_n'\cos 2\theta + \left(n(n-2)\phi_n - \phi_n''\right)\frac{\sin 2\theta}{2}\right),\\
\frac{\partial u_x^{NS}}{\partial y} &= \frac{1}{r}\sum_{n=1}^{+\infty}\left(\frac{r}{\nu}\right)^{n-1}\left((n-1)\phi_n'\sin 2\theta + n(n-1)\phi_n\sin^2\theta + \left(n\phi_n + \phi_n''\right)\cos^2\theta\right).
\end{aligned} \tag{117.}$$

E. Calculation of p^{NS}

By using the expressions (27) and (34), as well as formula (22), we get:

$$\begin{aligned}\omega^{NS}\frac{\partial\phi^{NS}}{\partial r} &= \frac{1}{\nu}\left(\sum_{n=0}^{+\infty}\left(\frac{r}{\nu}\right)^{n-1}\omega_{n-1}\right)\left(\sum_{n=0}^{+\infty}(n+1)\left(\frac{r}{\nu}\right)^{n}\phi_{n+1}\right) = \frac{1}{r}\sum_{n=0}^{+\infty}\left(\frac{r}{\nu}\right)^{n}A_n,\\ \omega^{NS}\frac{\partial\phi^{NS}}{\partial\theta} &= \left(\sum_{n=0}^{+\infty}\left(\frac{r}{\nu}\right)^{n-1}\omega_{n-1}\right)\left(\sum_{n=0}^{+\infty}\left(\frac{r}{\nu}\right)^{n+1}\phi'_{n+1}\right) = \sum_{n=0}^{+\infty}\left(\frac{r}{\nu}\right)^{n}B_n,\end{aligned} \tag{118.}$$

with

$$A_n = \sum_{k=0}^{n}(n-k+1)\omega_{k-1}\phi_{n-k+1}, \quad B_n = \sum_{k=0}^{n}\omega_{k-1}\phi'_{n-k+1}, \quad \forall n\in\mathbb{N}. \tag{119.}$$

It is useful to note that

$$\frac{\partial\omega^{NS}}{\partial r} = \frac{1}{\nu^2}\sum_{n=-1}^{+\infty}\left(\frac{r}{\nu}\right)^{n-1}n\omega_n. \tag{120.}$$

Then the system (71) leads to

$$\begin{aligned}\frac{\partial p_d^{NS}}{\partial r} &= -\frac{\nu}{r^2}\omega'_{-1} - \frac{1}{\nu}\sum_{n=0}^{+\infty}\left(\frac{r}{\nu}\right)^{n-1}(\omega'_n + A_n),\\ \frac{\partial p_d^{NS}}{\partial\theta} &= -\frac{\nu}{r}\omega_{-1} + \sum_{n=0}^{+\infty}\left(\frac{r}{\nu}\right)^{n}(n\omega_n - B_n).\end{aligned} \tag{121.}$$

By integrating the first equation, we immediately obtain

$$p_d^{NS}(r,\theta) = \frac{\nu}{r}\omega'_{-1} - \ln r(\omega_{-1}\phi_1 + \omega'_0) - \sum_{n=1}^{+\infty}\left(\frac{r}{\nu}\right)^{n}\frac{\omega'_n + A_n}{n} + f(\theta). \tag{122.}$$

By deriving now (122) with respect to θ and by identifying with the expression of $\frac{\partial p_d^{NS}}{\partial\theta}$ from (121), we obtain $f'(\theta) = -\omega_{-1}\phi'_1$. We can thus calculate p_d^{NS} up to a constant. Finally, let us note that

$$\boldsymbol{u}^{NS}\cdot\boldsymbol{u}^{NS} = \frac{1}{r^2}\left(\frac{\partial\phi^{NS}}{\partial\theta}\right)^2 + \left(\frac{\partial\phi^{NS}}{\partial r}\right)^2 = \left(\sum_{n=0}^{+\infty}\left(\frac{r}{\nu}\right)^{n}\phi'_{n+1}\right)^2 + \left(\sum_{n=0}^{+\infty}\left(\frac{r}{\nu}\right)^{n}(n+1)\phi_{n+1}\right)^2, \tag{123.}$$

such that

$$\boldsymbol{u}^{NS}\cdot\boldsymbol{u}^{NS} = \sum_{n=0}^{+\infty}\left(\frac{r}{\nu}\right)^{n}C_n, \qquad C_n = \sum_{k=0}^{n}\phi'_{k+1}\phi'_{n-k+1} + (k+1)(n-k+1)\phi_{k+1}\phi_{n-k+1}. \tag{124.}$$

A simple calculation yields:

$$p^{NS}(r,\theta) = \frac{\nu}{r}\omega'_{-1} - (\omega_{-1}\phi_1 + \omega'_0)\ln r - F(\theta) - \sum_{n=1}^{+\infty}\left(\frac{r}{\nu}\right)^{n}\left(\frac{\omega'_n + A_n}{n} + \frac{C_n}{2}\right), \tag{125.}$$

where

$$F(\theta) = \frac{1}{2}\left((\phi'_1)^2 + \phi_1^2\right) + \int\omega_{-1}\phi'_1\,d\theta. \tag{126.}$$

One may note that $(\omega_{-1}\phi_1 + \omega_0')' = 0$, according to (98), and that $F'(\theta) = \phi_1'(\phi_1'' + \phi_1 + \omega_{-1}) = 0$. Thus, we have that $F(\theta)$ is constant and also that:

$$\omega_{-1}\phi_1 + \omega_0' = \frac{2\pi^4 + 25\pi^2 - 44}{8(\pi^2 - 4)^2} =: K. \qquad 127.$$

We finally get that

$$p^{NS}(r,\theta) = \frac{\nu}{r}\omega_{-1}' - K\ln r - \sum_{n=1}^{+\infty}\left(\frac{r}{\nu}\right)^n\left(\frac{\omega_n' + A_n}{n} + \frac{C_n}{2}\right) + c, \quad c \in \mathbb{R}. \qquad 128.$$

LITERATURE CITED

Becker R, Capatina D, Luce R, Trujillo D. 2015a. Finite element formulation of general boundary conditions for incompressible flows. *Computer Methods in Applied Mechanics and Engineering* 295

Becker R, Capatina D, Luce R, Trujillo D. 2015b. Stabilized finite element formulation with domain decomposition for incompressible flows. *SIAM Journal on Scientific Computing* 37:1270–1296

Blasius H. 1908. Grenzschichten in Flüssigkeiten mit kleiner Reibung. *Zeitschrift für angewandte Matematik und Physik* 56:1–37

Blasius H. 1950. The boundary layers in fluids with little friction. Translation of "Grenzschichten in Flüssigkeiten mit kleiner Reibung" Zeitschrift für angewandte Matematik und Physik, Band 56, Heft 1, 1908. Technical Memorandum 1256, National Advisory Committee for Aeronautics

Burda P, Novotný J, Šístek J. 2012. Analytical solution of Stokes flow near corners and applications to numerical solution of Navier-Stokes equations with high precision, In *Conference Applications of Mathematics*. Institute of Mathematics AS CR, Prague

Çengel YA, Cimbala JM. 2006. Fluid mehanics: fundamentals and applications. McGraw-Hill series in mechanical engineering, 1st ed.

Dijkstra D, Kuerten JGM. 1993. Asymptotics and numerics for laminar flow over a finite flat plate, chap. 1. Nato Science Series C: Asymptotic and Numerical Methods for Partial Differential Equations with Critical Parameters. Kluwer Academic Publishers, 3–19

Evans GA, Blackledge JM, Yardley PD. 1999. Analytic methods for partial differential equations. Springer-Verlag. Springer Undergraduate Mathematics Series

Falkner VM, Skan SW. 1930. Some approximate solutions of the boundary layer equations. Reports and Memoranda n °1314, Aeronautical Research Committee

Gatski TB, Grosch CE. 1987. Numerical experiments on boundary-layer receptivity. in stability of time dependent and spatially varying flows. ICASE NASA LaRC Series. Springer-Verlag, 82–96

Prandtl L. 1905. Über Flussigkeitbewegung bei sehr kleiner Reibung, In *III International Mathematiker-Kongresses, Heidelberg 1904*, ed. L Druck und Verlag von B. G. Teubner, pp. 484–491

Prandtl L. 1928. Motion of fluids with very little viscosity. Translation of "Über Flussigkeitbewegung bei sehr kleiner Reibung" . Technical Memorandum 452, National Advisory Committee for Aeronautics

Tunney AP, Denier JP, Mattner TW, Cater JE. 2015. A new inviscid mode of instability in compressible boundary-layer flows. *Journal of Fluid Mechanics* 785:301–323

van Kármán T. 1921. Über laminare und turbulente Reibung. *Zeitschrift für Angewandte Mathematik und Mechanik* 1:233–252